Diploma Thesis

DYNAMIC MECHANICAL ANALYSIS IN SMALL DIAMETER ELECTROSPUN VASCULAR GRAFTS

carried out for the purpose of obtaining the degree of Master of Science (MSc or Dipl.-Ing. or DI), submitted at TU Wien, Faculty of Mechanical and Industrial Engineering, by

Nikolaos Politis

Mat.Nr.: 01130096

under the supervision of

Univ.Prof. Dipl.-Ing. Dr. techn. **Heinz-Bodo Schmiedmayer**
Institute of Mechanics and Mechatronics

And

Univ.Prof. Dipl.-Ing. Dr. **Heinrich Schima**
Ludwig-Boltzmann-Cluster for Cardiovascular Research
Center for Medical Physics and Biomedical Engineering Medical University of Vienna

_____

Signature

Affidavit

I declare in lieu of oath, that I wrote this thesis and performed the associated research myself, using only literature cited in this volume.

Vienna, 22nd May 2019

Signature

Acknowledgment:

I would like to dedicate this Master Thesis to my parents Maria and Giannis, who made it possible for me to complete this study by their diligence and their unconditional support throughout these years. Since I was a young kid, they ensured that nothing stood in the way of my urge to expand my knowledge horizons. Also, from the time I moved in Vienna for my Master studies, they did what they could in order to make the study process much easier for me, even when that included the packages of Greek food and pastries from my homeland.

I would also like to thank my brother Stavros for his support and continuous supply of courage. As a brother and a friend, he always stood at my side at good and especially at bad times.

In the view of their dedication to research in the field of cardiovascular dynamics and artificial organs, I would like to thank all of my colleagues in the Center for Medical Physics and Biomedical Engineering, Medical University of Vienna. I would like to thank my fellow student BSc. Alex Maurer, who has become a very good friend of mine because of the time we spent together as students and his willingness to deal conscientiously with my questions.

I would particularly like to thank my supervisors A.o. Univ.-Prof. Dipl.-Ing. Dr. techn. Heinz-Bodo Schmiedmayer and A.o. Univ.-Prof. Dipl.-Ing. Dr. Heinrich Schima, for making this work possible. Without their support and their great guidance, I would not be able to gain all this knowledge. Last but not least I want to thank Dipl.-Ing. (FH) Martin Stoiber for all the time he spent to guide me, through the path of my thesis.

Abstract

Small diameter vascular grafts out of electrospun material offer a close match to the biomechanical and structural properties of native blood vessels. For an optimal adaptation of electrospun prostheses to native vessels, the mechanical behaviour as it would occur in vivo has to be predicted. Dynamic measurements are therefore favourable.

Aim of this work was to establish a protocol for performing force controlled dynamic mechanical analysis (DMA) measurements for dynamic characterisation, at physiological pressure range, by the use of DMA setup and common dynamic loading. Furthermore, common dynamic tests were performed in order to compare the information gained between these tests and DMA measurements.

For the experiments, five electrospun grafts of three different wall-thicknesses (w.t) (150, 200, 300μm) with inner diameter of 3 mm were prepared. A BOSE® Electroforce system (TA Instruments – ElectroForce Systems Group, New Castle, DE, USA) was used for tensile tests on ring-shaped specimens. The rings were loaded in circumferential direction by two steel pins. First, the specimens were loaded dynamically at force controlled mode by triangle and sinus waves. The dynamic loading consisted of 10 working cycles at frequency of 1Hz from 0.05N to 0.18N, corresponding to a physiological pressure of 50 to 150mmHg. Then, the samples were loaded in DMA mode with a logarithmic frequency sweep with 10 points from 1 to 100 Hz, with mean level of 0.18N, dynamic amplitude of 0.15N and a mean level rate of 0.1N/sec.

The dynamic tests for both triangle and sinus waves showed differences in the resulting force-displacement graphs. From the force-displacement graphs the stress-strain curves were produced by implementing two different approaches for strain calculation of circular grafts. From the stress-strain curves the elastic modulus was calculated. Grafts of 150μm had an E-modulus of 0.20MPa, whereas for 200μm and for 300μm the stiffness was 0.18MPa and 0.13MPa respectively. The results from the DMA show the behavior of the samples over the varying frequency. DMA measurements provide a variety of metrics as results for structural characterization. The mean dynamic stiffness for the 150μm samples was 0.62N/mm, for 200μm 0.94N/mm and for 300μm 1.13N/mm. The area of the hysteresis loop decreased at higher wall thickness. Dissipated energy was 0.16N*mm for samples of 150μm w.t, 0.01N*mm for 200μm, and 0.1N*mm for 300μm. The phase angle was 8.5degrees for 150μm, 7degrees for 200μm, and 6.5degrees for 300μm. The DMA measurement also showed an increase in storage and loss stiffness at higher loading frequency.

The structural behavior of small diameter ring-shaped specimens was measured by DMA and common dynamic loading experiments. The measurements showed that DMA is applicable for small ring-shaped electrospun samples. The viscoelasticity at varying frequencies at physiological loading was obtained, which gives more detailed information about the frequency dependent dynamic behavior. This allows a better characterization of the basic structural behavior in comparison to common dynamic tests.

Contents

List of Figures

List of Tables

Chapter 1

Introduction

1.1 Electrospinning

1.1.1 Introduction to electrospinning

The increasing number of patients in need of artificial vessel implantation due to cardiovascular diseases highlights the necessity for artificial vascular grafts [1]. Vascular tissue prosthesis is currently regarded as one of the most promising and innovative solutions in order to overcome drawbacks related to small-diameter vascular substitutes.

Electrospinning is a valuable technique, which allows to fabricate nanofiber vascular grafts with tailored structural properties, which are able to mimic the functional characteristics of the natural extracellular matrix [2]–[4]. Furthermore, electrospinning allows the production of nanofibers from various materials, e.g. organics and inorganics in different configurations and assemblies. Promising materials for the fabrication of electrospun vascular grafts are polyurethanes. Polyurethanes are known for their superior tensile strength, elastic properties and biocompatibility [5][6].

1.1.2 The method of electrospinning

The fundamental principle of the electrospinning is to produce nonwoven fibers in nanoscale through an electrically charged jet of polymer solution. This method for the production of nanofibers was developed by Formhals [7] and has been studied thoroughly in the last decades [8]–[10]. An electrically charged high molecular weight polymer solution is introduced to an electric field. As a result, two forces will act on the solution, i.e an electrostatic repulsive force E and a capillary force that causes liquid particles to flock together to minimize the liquid surface tension γ. While the magnitude of the electric field increases, the surface charge of the drop also increases. When the repulsive force exceeds the surface tension, the solution will break apart in long tiny liquid columns. The high concentration of charged particles of similar nature causes them to be stretched longitudinally. This tendency to stretch, along with jet inertia and rheology, will result in a random lateral jet motion and elongation, resulting in a decrease of the jet radius down to several hundreds of nanometers.

The basic idea behind the electrospinning process is the application of electrostatic forces to produce electrically charged jets out of polymer solutions. The basic setup of an electrospinning process requires three main components: The syringe (1) which contains the polymer solution, a high-voltage power supply (2) and a conductive rotating mandrel to collect the nanofibers (3) (**Figure 1.1**).

During the electrospinning process, the polymer solution is pumped out of the syringe through the needle with an accurate stable-rate infusion pump. Small drops of the solution are formed at the needle tip. These drops are charged by the application of high voltage directly onto the needle. The electric field between the needle and the collecting mandrel results in repulsive

forces that are greater than the surface tension of the polymer solution. The fluid jet is ejected from the needle tip toward the collector mandrel which is already spinning and oscillating simultaneously. The electric field contributes also to the stretching of the polymer jet, resulting to thinner fibers[11].

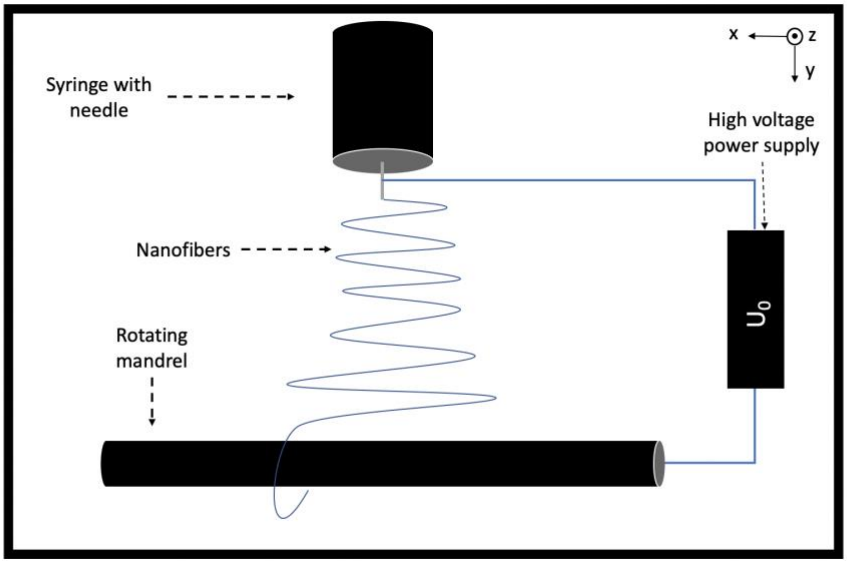

Figure 1.1: Top view of a basic electrospinning setup with its components. The electrodes generate a strong force that drag the nanofibers from the tipple of the needle to the target.

1.1.3 Parameters influencing electrospun grafts

There are publications in the literature that prove that there is a number of parameters influencing the morphology and properties of the electrospun grafts. These parameters can be divided in three main categories: solution properties, processing conditions and ambient conditions [12]-[11]. An overview of those parameters is presented in **Table 1.1**.

Table 1.1: Parameters influencing the electrospun grafts.

Solution Properties	Processing Conditions	Ambient Conditions
Viscosity	Applied voltage	Temperature
Polymer concentration	Tip to collector distance	
Molecurar weight of polymer	Flow rate	Atmospheric pressure
Electrical conductivity	Needle diameter	
Elasticity of polymer	Rotating and oscillating speed of the collector	Humidity
Solvent ratio of components		

Due to the low blood velocity into small vessels, graft material, structure and proper design are very important factors that should be taken into account [15]. The ideal small-diameter vascular graft must possess several characteristics, such as: (a) mechanical strength, which includes physiological compliance and no susceptibility to permanent creep that can lead to aneurysm formation; (b) biocompatibility, which is associated with a coalescent non-activated endothelium; (c) an acceptable healing response that does not result in inflammation, hyperplasia or fibrous capsule formation; and (d) ease of handling at the surgical standpoint [16].

The electrospinning method provides the opportunity to process a wide range of polymers in order to produce small-diameter blood vessels with tailored microstructural and mechanical properties [17].

1.2 Dynamic mechanical analysis

1.2.1 Introduction

A crucial part for designing and manufacturing vascular grafts with the electrospinning method is the in-vitro biomechanical characterization of these electrospun grafts. Due to the nature, the size and the viscoelastic behavior, most of the common mechanical tests have drawbacks and are unable to provide reliable results. To achieve the best possible characterization, there is a clear need for DMA, additional to the established quasi-static tests.

DMA is becoming more and more frequently seen in the analytical laboratories as a tool [18]–[20]. This technique is still treated with hesitation from a small number of scientists, due to the fact that is based on the field of rheology. Rheology is the study of the deformation and flow of materials. DMA is a technique that does not require a lot of specialized training to be used for material characterization. It allows the characterization of bulk properties directly affecting the performance of the structure or the material and has as a basic principle the application of an oscillating force to a sample and the measurement of the strain that occurs.

1.2.2 Basic principle of DMA

DMA is based on applying an oscillating force to a specimen and measuring the response of the material to the applied force. With this method, it is possible to calculate material properties such as viscosity from the phase angle and the stiffness from the recovery of the specimen. These properties resemble the capability of a material to dissipate energy (damping) and to recover from the deformation (elasticity).

If a force (F) is applied across an area (A) of a specimen the quotient of force divided by area is called stress (σ). When subjected to a stress, a material will exhibit a deformation or strain, ε. This relation is usually visualized through stress-strain curves. The slope of the stress-strain curve is the modulus, which is a measurement of how stiff is the material being tested. The modulus of a material is an indication of its performance in a real-world application. These data traditionally were derived from mechanical quasistatic tensile tests.

However, the measured modulus in DMA is not exactly the same as the modulus obtained by the classic stress-strain curves from tensile tests (**Figure 1.2**). DMA measures the material response to the applied sinusoidal force wave and calculates a complex modulus (E*), a storage modulus (E’), a loss modulus (E’’), the phase shift between storage and loss modulus (Phase Angle), and the elastic hysteresis. These different moduli enable a better characterization of the material because we can quantify the ability to recover energy (E’), to lose energy (E’’) and the damping (tan δ) which is the ratio of these effects (**Figure 1.3**). Phase angle is the measurement of phase lag between the implemented force wave and the measured displacement, and elastic hysteresis is a measurement of the dissipated energy.

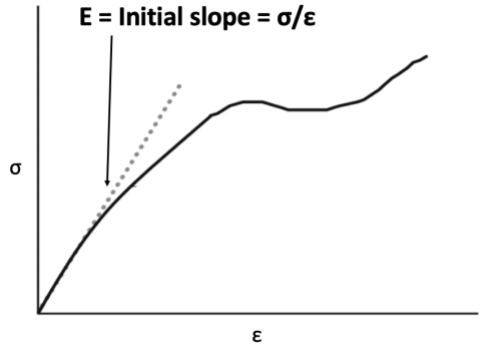

Figure 1.2: A typical stress-strain curve from a tensile experiment. The ratio between stress and strain in the initial linear region is the Young's Modulus.

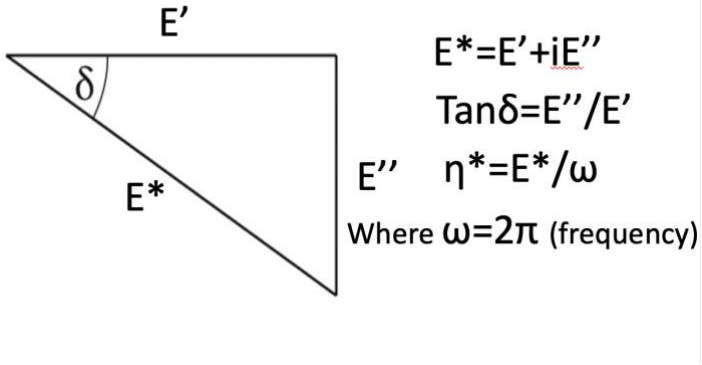

Figure 1.3: The modulus, the viscosity and the damping are calculated by measuring the amplitude of the strain at the peak of the sine wave, and the phase shift (δ) between stress and strain waves. The more elastic the material the more E' approaches E*.

1.2.3 Applying a dynamic stress to a sample

If we apply an oscillating load at a sample, we equivalently apply a sinusoidal stress wave. Then we can expect that the applied stress can be defined as

$$\sigma = \sigma_0 \sin(\omega t) \tag{1.1}$$

where σ is the stress at time t, σ_0 is the stress amplitude, and ω is the angular frequency of oscillation. Depending on the material and on its viscous behavior as well as elastic behavior, the resulting strain wave will have a phase shift δ from the applied stress wave. If the material is at the elastic limit (Hookean limit) then it will reply elastically on the applying stress, and the strain wave should be in phase (δ=0) with the stress wave. If the applied stress is in the linear elastic region, then σ and ε are linearly related by the Elastic Modulus E, and the strain response can be written as

$$\varepsilon(t) = \varepsilon_0 \sin(\omega t) \tag{1.2}$$

where ε_0 is the strain amplitude. This can be seen in **Figure 1.4a**, where there is no phase shift between the stress and the strain curve. If we now examine a material with a viscous behaviour, the stress is proportional to the strain rate. The viscous response can be expressed as

$$\varepsilon(t) = \eta \frac{d\sigma_0}{dt} = \eta\omega\sigma_0 \cos(\omega t) \tag{1.3}$$

or

$$\varepsilon(t) = \eta\omega\sigma_0 \sin(\omega t + \pi/2) \tag{1.4}$$

where η is the viscosity, and the equation can be written as

$$\varepsilon(t) = \omega\varepsilon_0 cos(\omega t) = \omega\varepsilon_0 \sin(\omega t + \pi/2) \tag{1.5}$$

This behavior can be seen in **Figure 1.4b**. Any other case with viscoelastic material behavior between the elastic and the viscous limits will be intermediate between the aforementioned cases and is shown in **Figure 1.4c**.

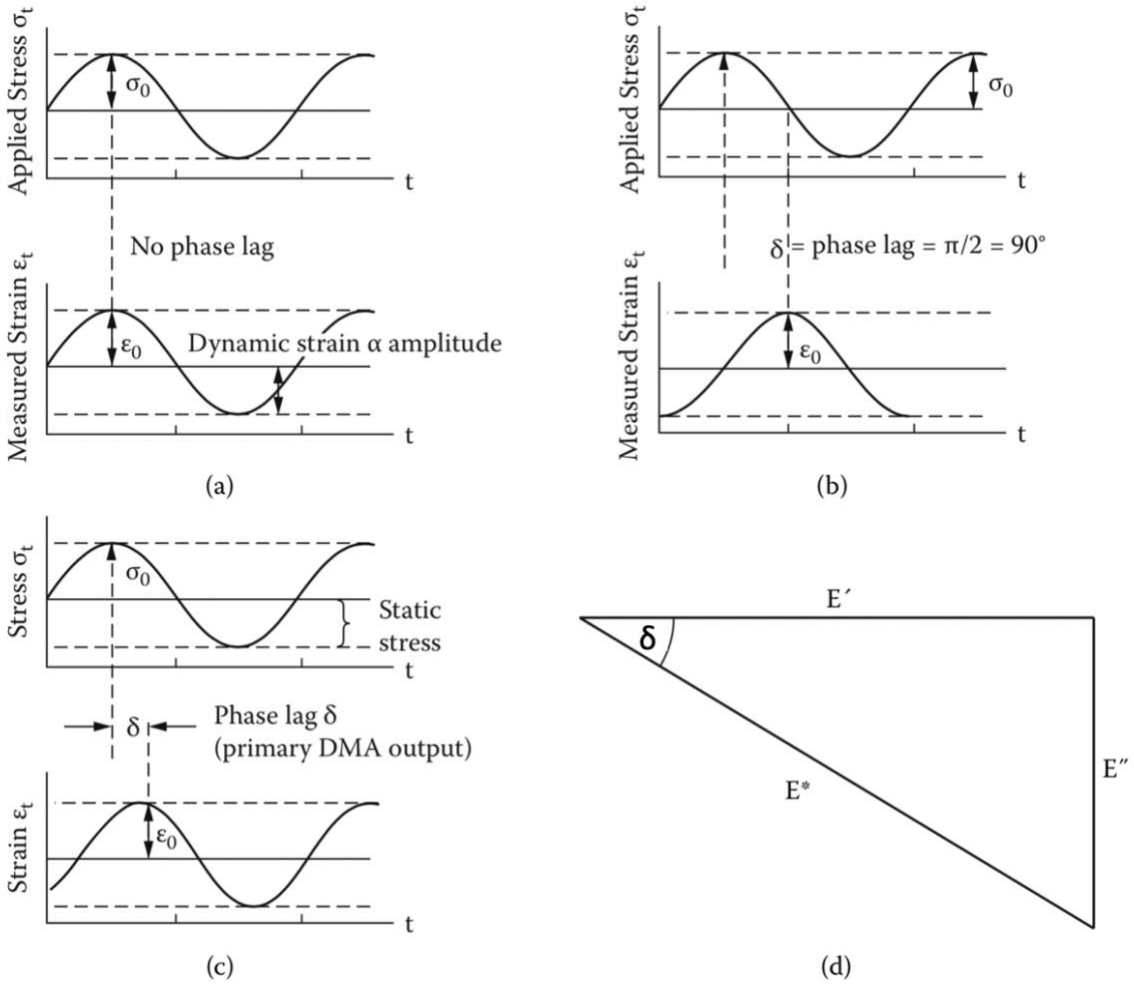

Figure 1.4: (a) No phase shift is observed between the applied wave and the measured wave when the material is perfectly elastic, (b) on the other hand when the material is perfectly viscous the response is out-of-phase to the applied wave. (c) Response of viscoelastic materials. The relationship between phase angle (δ), E*, E´ and E''. [21]

The difference between the applied stress and the resulting strain is the phase angle δ and when added to the strain equation (1.2), the elastic response of the material at any time can be expressed as

$$\varepsilon(t) = \varepsilon_0 \sin(\omega t + \delta). \tag{1.6}$$

The tangent of the phase shift is one of the most important properties calculated in DMA. It is the ratio of the loss modulus (E'') to the storage modulus (E') and is independent of geometry effects. This is called damping and it deflects the efficiency with which the material loses energy to molecular rearrangements and internal friction.

$$\tan \delta = E''/E' \tag{1.7}$$

where

$$E'' = \text{Loss Stiffness} = \frac{\sigma_0}{\varepsilon_0} \sin \delta \tag{1.8}$$

and

$$E' = \text{Storage Stiffness} = \frac{\sigma_0}{\varepsilon_0} \cos \delta \tag{1.9}$$

calculated based on the

$$E^* = \text{Dynamic Stiffness} = E' + iE'' \tag{1.10}$$

returned by the Fourier analysis as the ratio of the measured channel and the reference channel (typically force and displacement).

1.3 Objective of thesis

The main objective of this thesis is to establish DMA measurements for small-diameter electrospun grafts and establish a protocol for performing force controlled DMA meaurements that will be reproducible from any future user of the BOSE ElectroForce testbench system. Moreover, the additional value of DMA in structural properties will be investigated. The optimal dynamic characterization of the ring-shaped samples will be done by the use of DMA measurements at physiological pressure range and the use of common dynamic loading experiments. In particular, DMA experiments will be performed to measure the structural properties of materials as function of increasing frequency.

To allow a more generic understanding of the structural behavior of the small-diameter grafts made by the electrospinning method, the influence of wall thickness of the electrospun grafts will be studied also, by comparing the differences between the results of DMA measurements and dynamic loading. The process for the production of the electrospun prostheses and the steps followed, together with the parameters for the mechanical testing of the grafts, will be presented in chapter 2. Finally, the goal is to compare the gained information from the DMA measurements with the results from common dynamic tensile testing and report the differences of both experiments in chapter 3.

Chapter 2

Materials & Methods

2.1 Mechanical testing setup

The circumferential strength of the electrospun grafts was measured with the BOSE ElectroFroce® TestBench LM1 system (Bose Corp. MN, USA) modified for tensile tests on ring-shaped specimens. This system is configured with a controllable linear motor which can produce forces up to 200N and a 10N force transducer. The displacement range of the linear actuator is 13mm, from -6.5mm to 6.5mm. Specifications of the testing systems can be seen in **Table 2.1** and the experimental setup is shown in **Figure 2.1**. It consists of a moving, and a static part. One pin is attached to the moving part of the linear motor and controls the displacement, while the other pin is attached to the static part and connected with a load cell to control the force. The rings were loaded in circumferential direction by two steel pins with diameter of 0.6 mm.

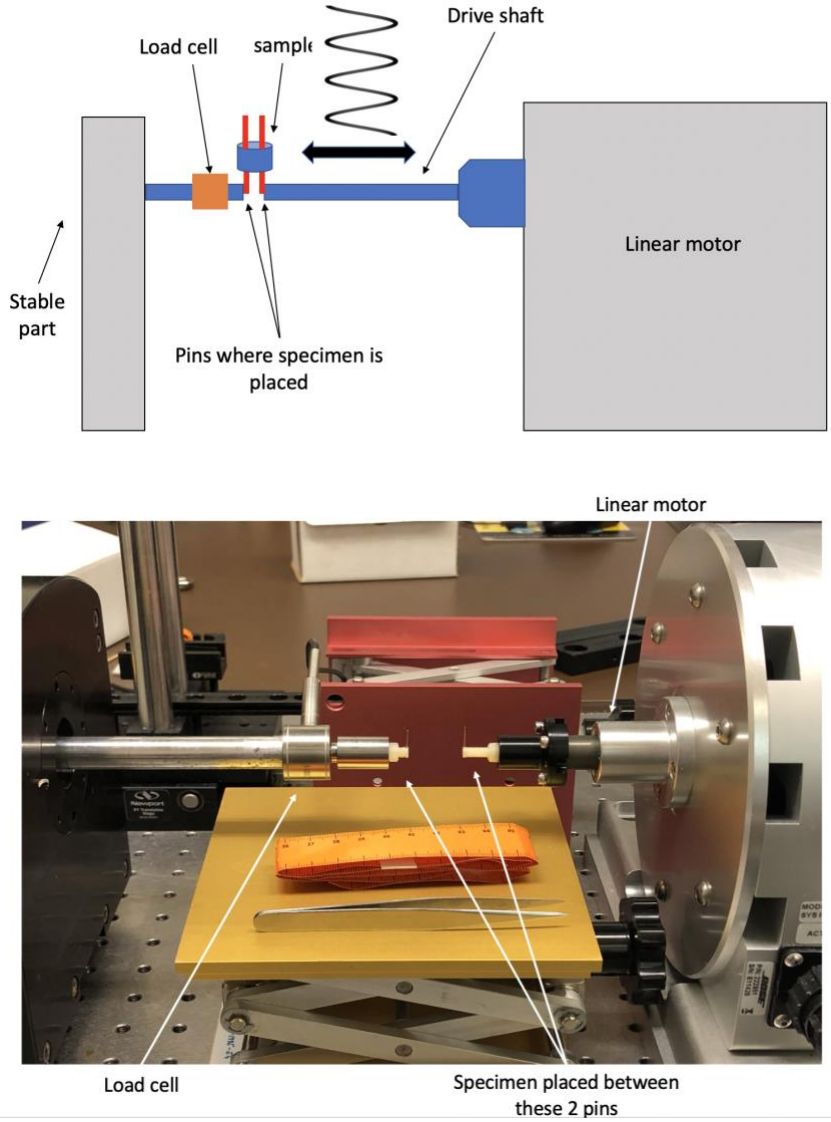

Figure 2.1: Modified tensile testing machine.

Table 2.1: Specifications of BOSE ElectroForce® TestBench LM1 system [22].

Typical TestBench Component Specifications*					
	Peak Force/ Torque	Stroke/ Rotation	Maximum Velocity‡	Approximate Dimensions (H x W x L)	Approximate Weight
ElectroForce 200 N	± 200 N (± 45 lb)	± 6.5 mm (± 0.25 in)	3.2 m/s (126 in/s)	216 x 280 x 254 mm (8.5 x 11 x 10 in)	7.3 kg (16 lb)

2.2 Electrospinning tubular scaffolds

The vascular grafts were fabricated with an electrospinning device comprising a high-voltage power supply (CPP 300-304-24-5, ET System electronic GmbH, Altlussheim, Germany), a custom-made infusion pump, a syringe, and a rotating mandrel (**Figure 2.2)**. The 2-mL syringe held the polymer solution and was fitted with a blunt-ended needle which was connected to the high voltage generator. The polymer solution was pumped through the syringe. All grafts were made of 4% Pelletane 2363-80A. The mandrel (diameter: 3.0 mm, length: 98 mm) was rotated at 250 rpm and oscillated in the transverse direction. The distance between the needle and the mandrel was set at 9 cm. The polymer solution was electrostatically drawn from the tip of the needle by applying a voltage of 9 kV to the mandrel. The complete electrospinning device was placed in a Faraday cage and operated in a class 1000 clean room at a temperature of 26°C and a relative humidity of 28% [17]. An example of an electrospun mandrel can be seen in **Figure 2.3**.

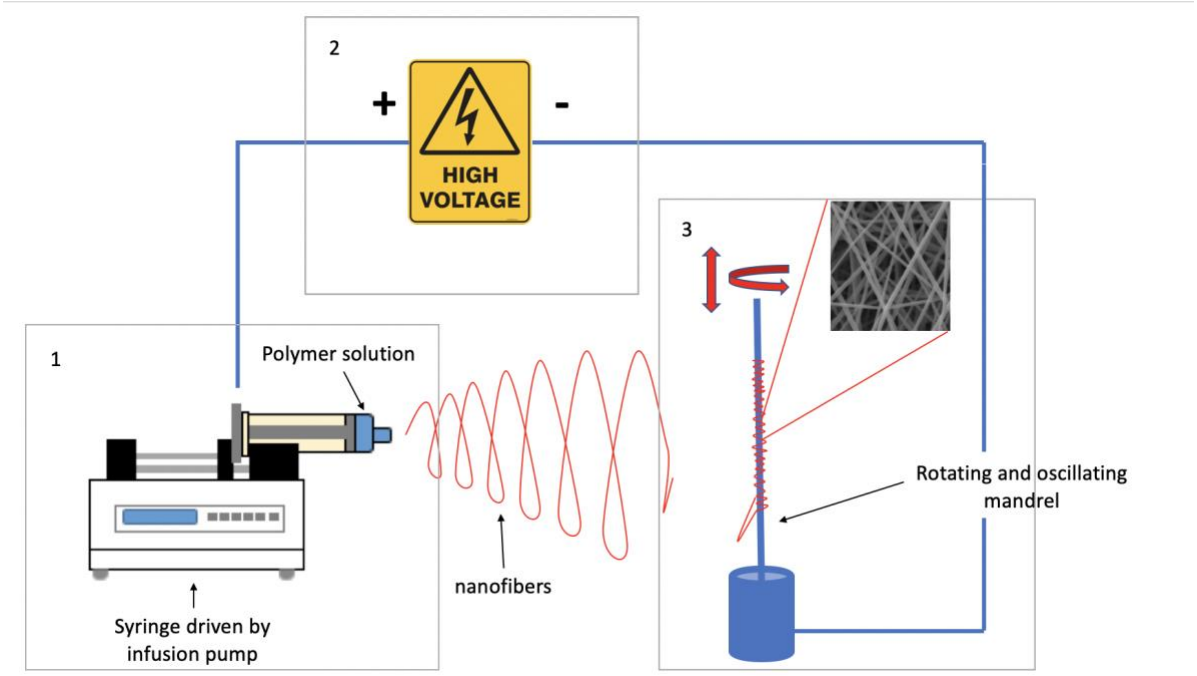

Figure 2.2: Basic scheme of electrospinning - (1) syringe and infusion pump, (2) high voltage power supply, (3) collecting mandrel. The tip of needle is connected to high voltage and the ground was connected directly at the rotating mandrel. The rotating and oscillating mandrel collects the fibers and is positioned between these two electrodes.

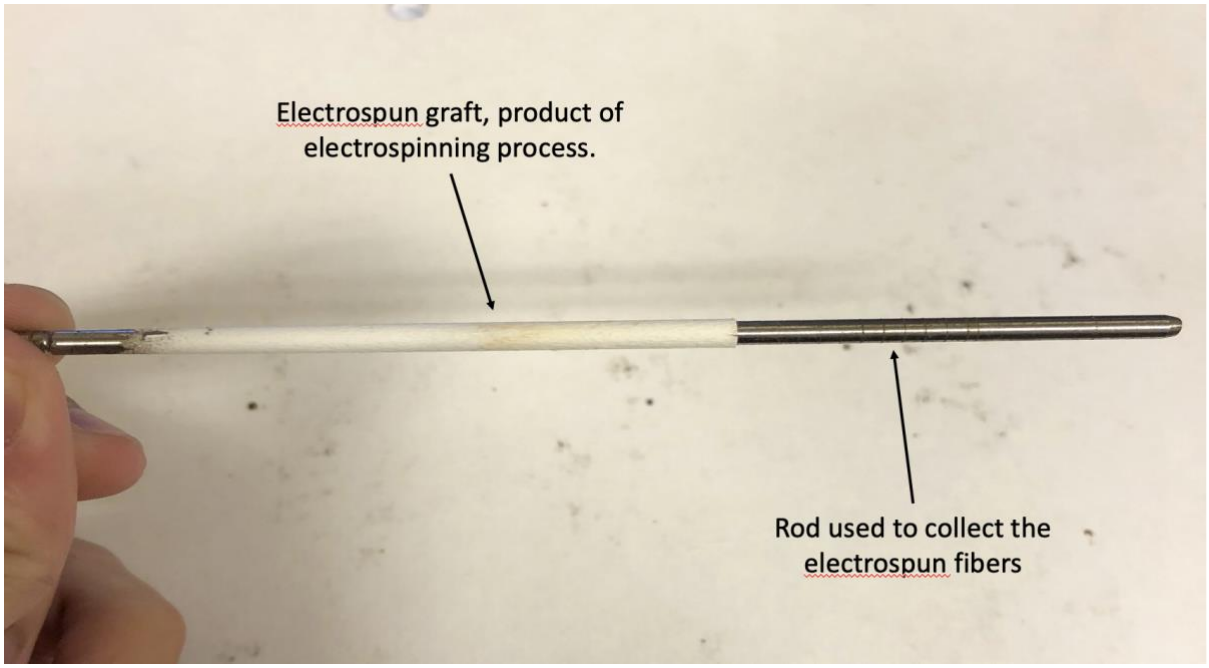

Figure 2.3: An example of finished electrospun mandrel.

Using the method described above, three electrospun grafts with a 3.0 mm inner diameter and 98 mm length, and 3 different wall thicknesses of ~150 µm, ~200 µm and ~300 µm were manufactured. The inner diameter of the grafts was limited by the size of the mandrel and the wall thickness by the spinning time. In order to produce grafts with different wall thickness, each rod was spun for a different amount of time. The spinning time of each rod and the resulted wall thickness can be seen in **Figure 2.4** and **Figure 2.5**.

Specimens			
	#1	#2	#3
Electrospun time	25 min.	45 min.	70 min.
Wall Thickness [µm]	100-150	170-250	260-340

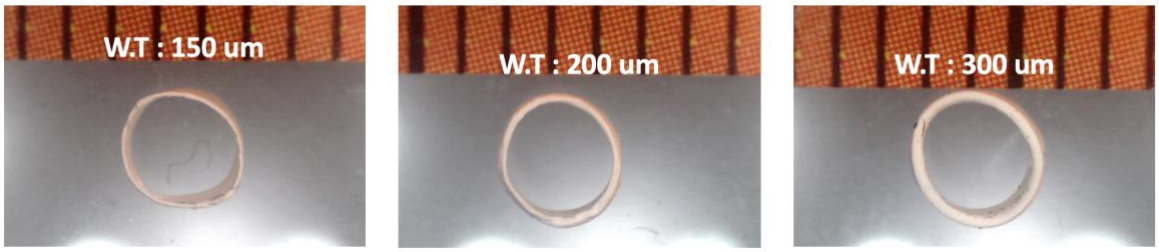

Figure 2.4: Varying electrospun time and the resulting wall thickness.

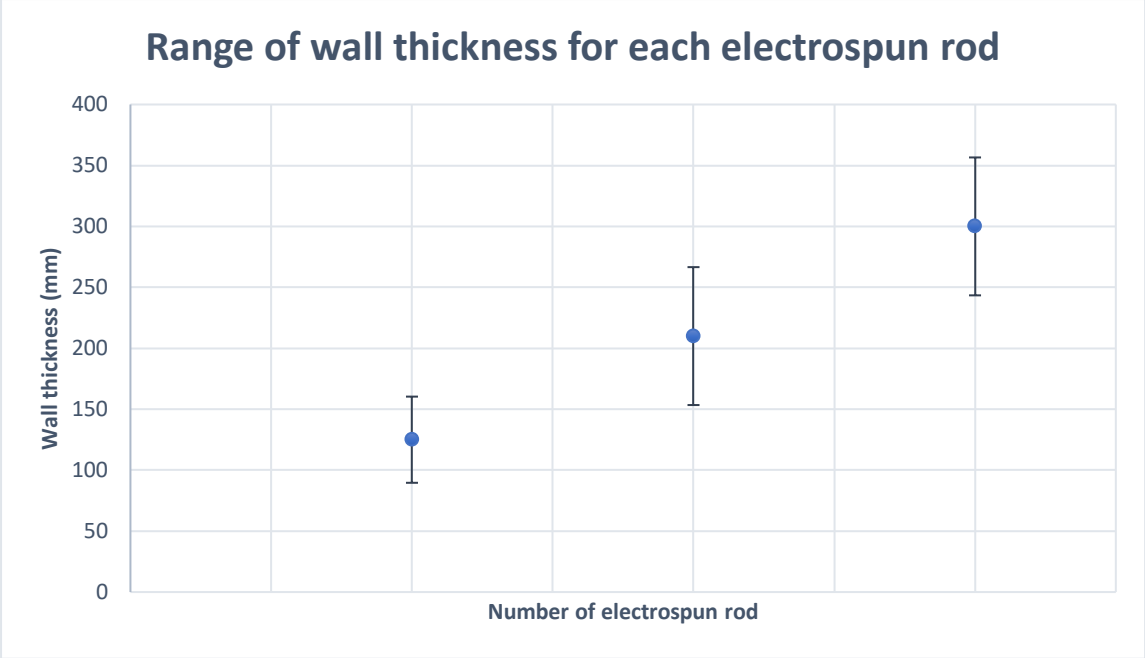

Figure 2.5: The resulted range wall thickness for each rod across the whole length that was spun.

2.3 Examination of wall thickness and selection of specimens

The electrospun mandrels were dried under vacuum at room temperature for 24 h. The outer diameter of each rod was measured with a non-contacting optical micrometer (ODC 2600, MICRO-EPSILON Eltrotec GmbH, Uhingen, Germany). The measurement system consists of a light source, a receiver and the controller. The measurement setup can be seen in **Figure 2.7**. The receiver is an integral high-resolution line-scan camera for the measurement of geometrical quantities. The light source illuminates the target from the rear. The line scan camera in the receiver measures the projected outer contour of the target with resolution of 0.1 µm [23]. The measurement program "Diameter of a target" was selected as operating mode. The electrospun rod was then mounted on the mounting rail between the light source and the camera. During the measurement, the mounting rail is rotated and scanned, between the LED source and the receiver lens, across the whole length of the rod and the measurement of the diameter of the target is obtained. The working principle of the optical micrometer is shown in **Figure 2.6**.

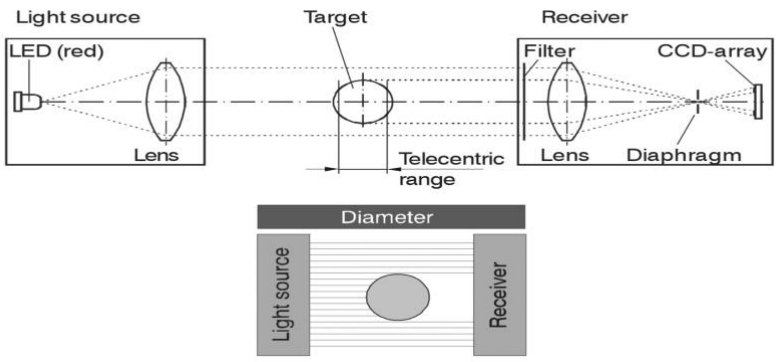

Figure 2.6: Mesuring principle of optical micrometer. [23]

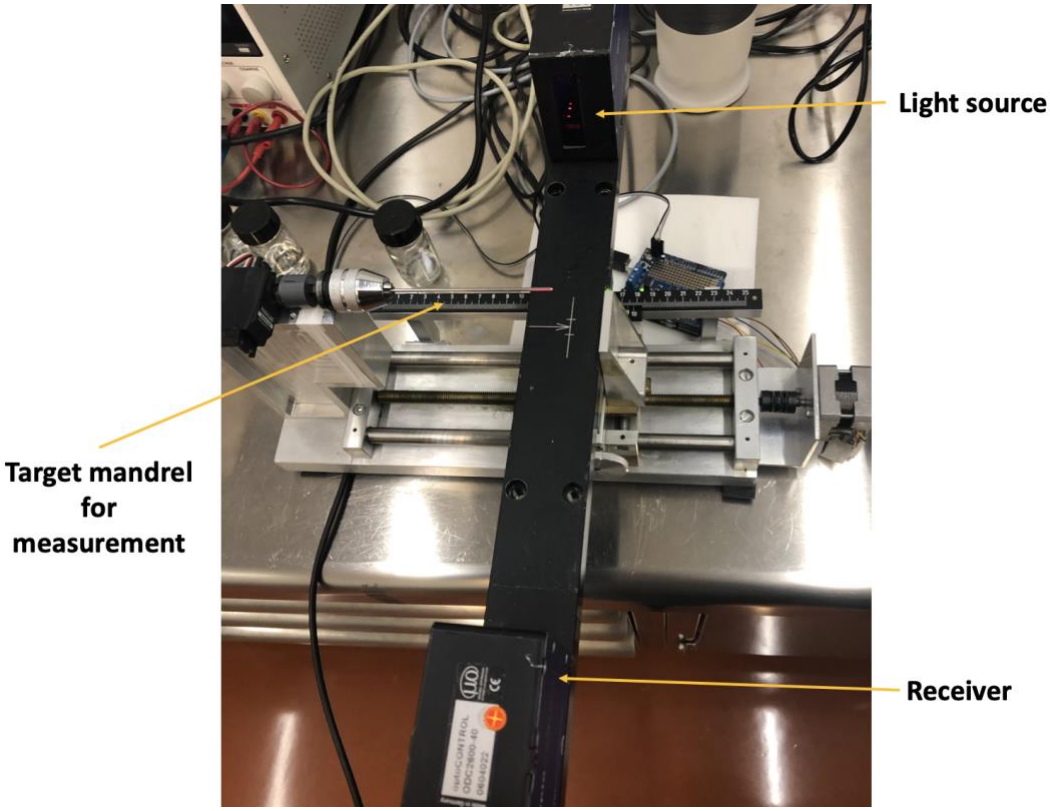

Figure 2.7: The optical micrometer measurement system and its components [23].

The outer diameter of each electrospun rod was measured, careful selection of the specimens was done at the zone of the rod, where the wall thickness had lower variation from the desired values. The zone chosen for each rod can be seen in **Figure 2.8**.

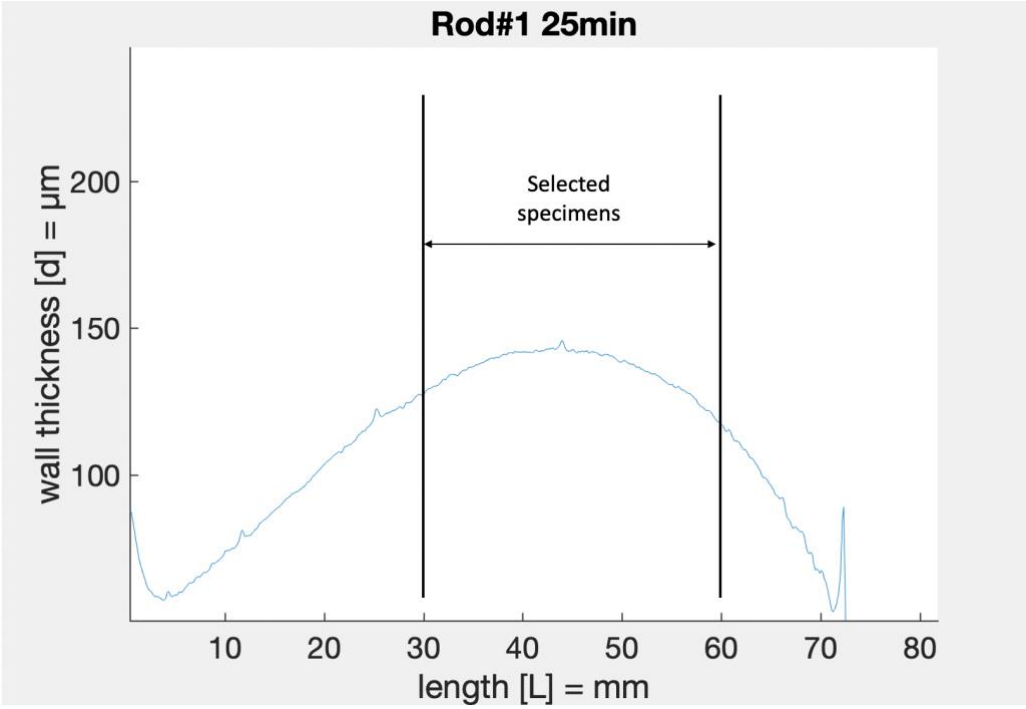

(A)

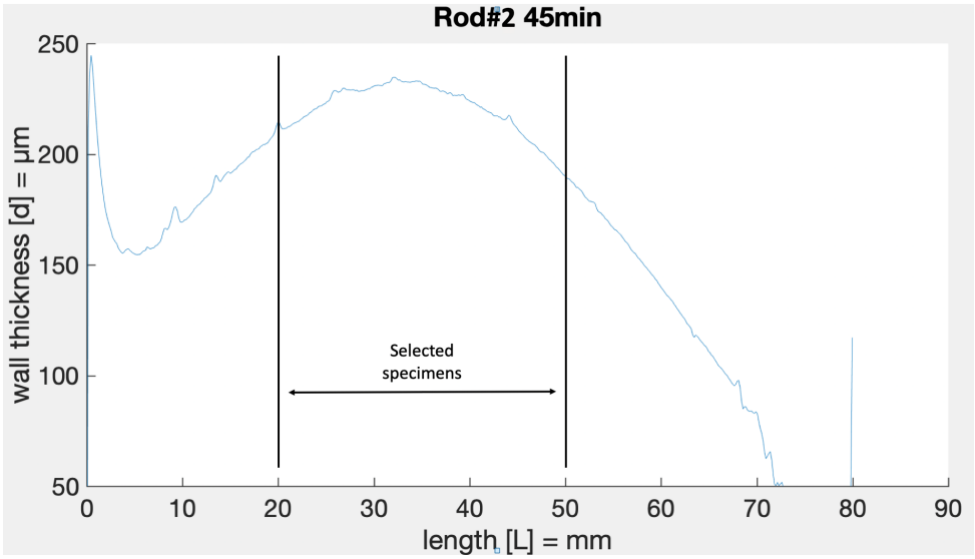

(B)

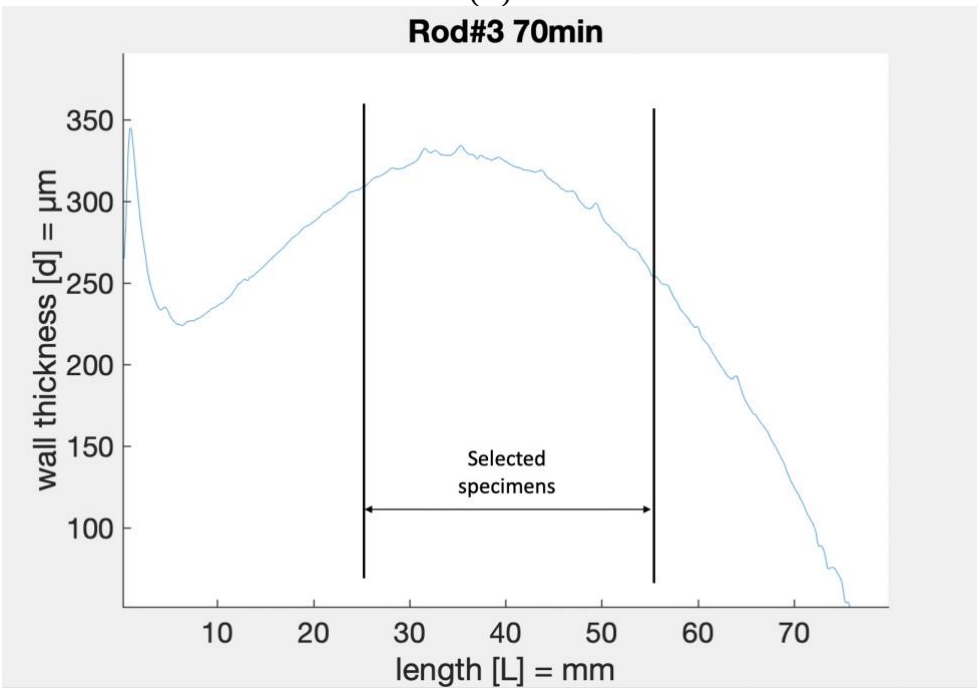

(C)

Figure 2.8: Selected zone for extraction of specimens. (A) For the mandrel with wall thickness of 150 µm, (B) and (C) are for the mandrels with 200 µm and 300 µm wall thickness respectively.

For each wall thickness, 6 specimens for the open angle experiments and 6 specimens for the application of DMA measurements were prepared. The grafts for the mechanical tests had a length of 3mm, while the grafts used for the open angle experiments had a length of 2mm. The specimens were cut precisely with a lathe using a knife as it can be seen in **Figure 2.9**. The specimens were cut alternating for the mechanical tests and the open angle experiments. For example, in the rod with wall thickness 150µm the first set of specimens were cut from 30-35mm and contained both the first set of specimens for the mechanical tests and the open angle experiments. The same procedure was followed until both 5 sets of specimens were collected for each wall thickness. From these 6 specimens, 1 was used for preliminary tests, to optimize the procedure for the DMA application.

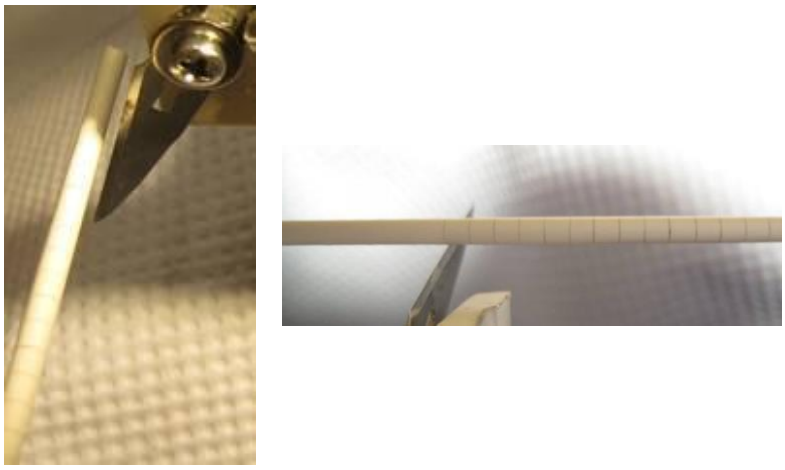

Figure 2.9: Self-made cutting knife used to cut the grafts precisely.

2.4 Open angle experiments

In order to examine if residual stresses are present on the electrospun grafts open angle experiments were performed, as proposed by Fung [24]. The Green's strains in circumferential direction ($E_{\theta\theta}$) are related to the corresponding stretch ratios (λ_θ) [25].

$$\text{Circumferential: } E_{\theta\theta} = \frac{1}{2}\left(\lambda_\theta^{\,2} - 1\right) \tag{2.1}$$

A photo of each ring was taken before performing an axial cut with a surgical knife. For each ring, an axial cut was made, thereby releasing residual stresses. After 30 minutes, a digital image of each ring was taken in order to determine the change of the geometry and measure the open angle and the change of length in the inner and outer circumference. A second digital image was made after 60 minutes to compare the measurements with the first image made at 30 minutes after the cut (**Figure 2.10**).

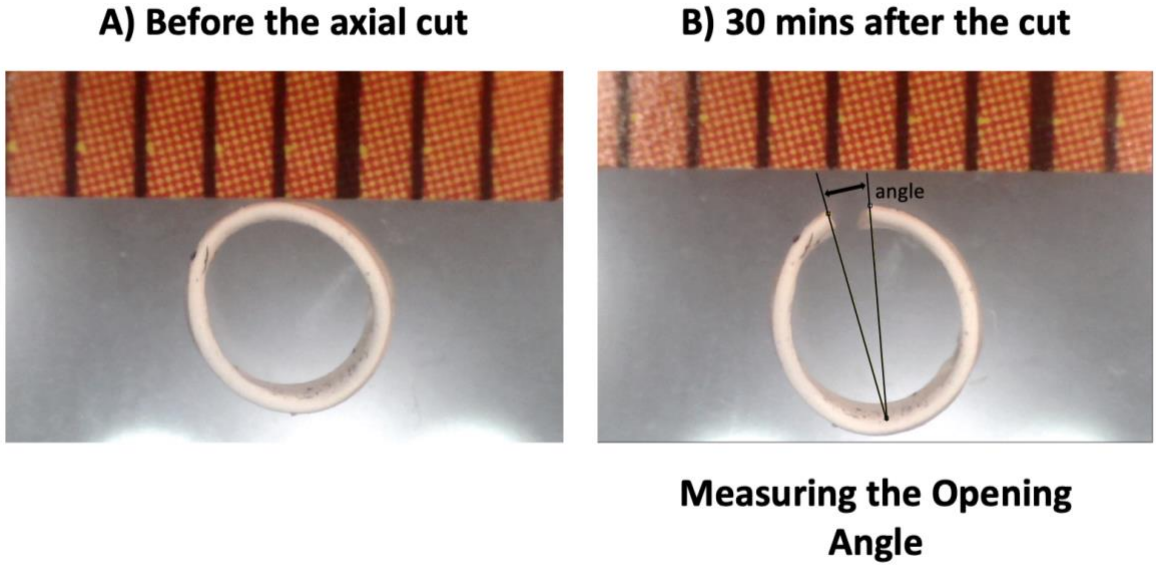

Figure 2.10: Images taken of a specimen with 300μm wall thickness before and after the axial cut. Measurement of Opening Angle is also shown according to [24].

The images taken were implemented in to the ImageJ (ImageJ 1.52a, National Institutes of Health Bethesda, USA) and the opening angle was measured on the middle point from the length of the inner circumference. The length of the circumference of the inner wall of the graft was measured before and after the axial cut

$$L^{i\theta}_{0\,stress}: length\ after\ the\ cut\ (zero-stress)$$
$$L^{i\theta}_{no\ load}: length\ before\ the\ cut\ (no-load\ state)$$

where superscripts i and θ are indicative of "inner" and "circumferential". Similarly, the circumferential length of the outer wall was measured and obtained:

$$L^{o\theta}_{0\,stress}: length\ after\ the\ cut\ (zero-stress)$$
$$L^{o\theta}_{no\ load}: length\ before\ the\ cut\ (no-load\ state)$$

From the measurements, we obtain the stretch ratios on the inner and on the outer wall.

$$\lambda^{i\theta}_{no\ load} = \frac{L^{i\theta}_{no\ load}}{L^{i\theta}_{0-stress}}\ (2.3)\ ,\ \lambda^{o\theta}_{no\ load} = \frac{L^{o\theta}_{no\ load}}{L^{o\theta}_{0-stress}}\ (2.4)$$

2.5 Deformation experiments

In order to quantify the effects of wall thickness into the mechanical measurements, one specimen from each wall thickness (150μm, 200μm, and 300μm) was deformed until the stretched position was reached like the schematic representation in **Figure 2.11**. The stretched position was reached when the distance of the walls is equal to the diameter of the pins d=0.6mm.

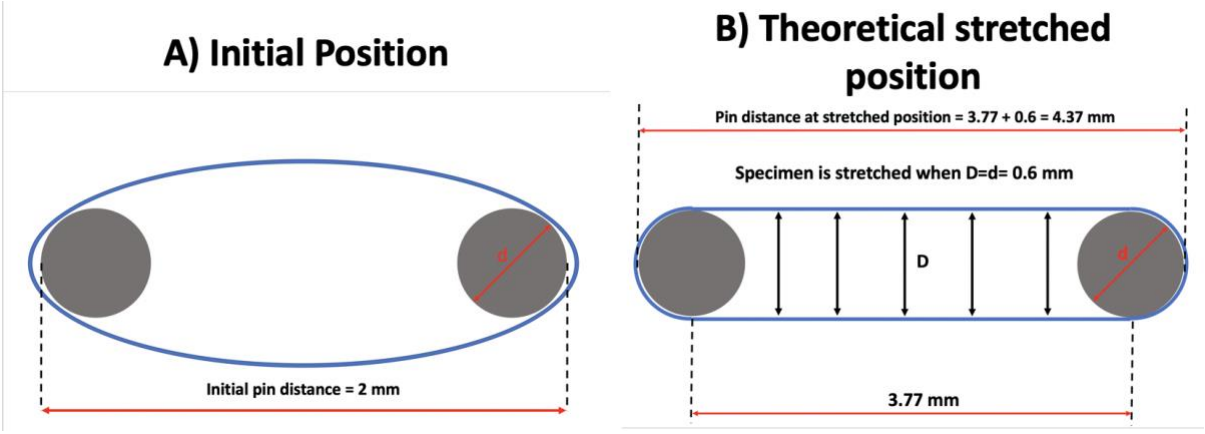

Figure 2.11: Schematic drawing of initial position, and the theoretical stretched position.

The initial distance between the two metallic pins was fixed at 2 mm. An image of the pins was made. The image was inserted in Image J, in order to achieve a correspondence between the pixels of the image and the length of a millimetre. After the distance was fixed, a specimen from each wall thickness was placed and deformed with a step of 0.1 mm until the stretch position was reached. In each step, a photo of the specimen was made so that the distance between the walls can be measured, and the deformation from the initial configuration to the stretched one can be seen. The generated force and displacement were measured during the deformation.

2.6 Calculation of force range

To investigate the mechanical properties of the ring-shaped specimens the testing machine used was the BOSE ElectroForce 200N testbench system, with the experimental setup described in Chapter 2.1. The testing machine is accompanied with the WinTest® software package. WinTest® is the user interface and control platform of the ElectroForce testbench. This software was used to implement first a triangular dynamic loading, then a sinusoidal dynamic loading and as a final step perform a dynamic mechanical analysis with a frequency sweep at a constant temperature.

All the experiments were performed in force control mode. This means that the control channel was the force and the measured channel was the displacement. The force range applied at the ring-shaped specimens was calculated, using Laplace's Law for thin-walled vessels. An assumption was made that the relevant stresses in the wall of the electrospun grafts are hoop stresses (assumption of a thin-walled vessel) (**Figure 2.12**).

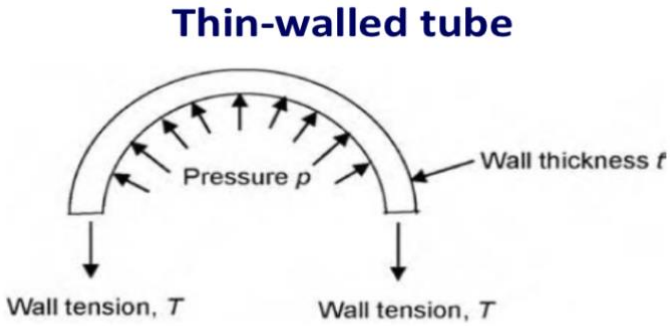

Figure 2.12: Thin-walled assumption for Force calculation of force range for DMA experiments.

$$F = T * A \quad , \quad T = p * \frac{D}{2*t} \quad , \quad A = 2 * t * l \tag{2.5}$$

where, T: wall tesnsion F: applied force, p: pressure, D: inner diameter, t: wall thickness, A: area and l: length of graft

From the physiological pressure range and the geometry of the electrospun grafts the Force range for the experiments was calculated (**Table 2.2**).

Table 2.2: Force range that corresponds to the physiological pressure range and used for the experiments.

Desired conditions		**Applied conditions**	
Pressure	**Force**	**Force**	**Pressure**
80 mmHg	0.096 N	0.03 N	28 mmHg
120 mmHg	0.143 N	0.35 N	285 mmHg

2.6.1 Measurement procedure

As mentioned in the objective of the thesis, one of the main tasks of this work was to establish a reproducible protocol for force-controlled DMA measurements. In this section, the procedure of the experiments will be explained thoroughly. The same workflow was followed and repeated for every specimen.

The first step of the procedure was to set the distance between the pins 2 mm. The specimen was installed in the experimental setup. For better optimization of the results the software provides an automatic tuning function called TuneIQ. TuneIQ uses Bose-proprietary tuning algorithms to provide automatic tuning for ElectroForce linear motors in both displacement and load control for nearly all tuning situations. To use TuneIQ with a cyclic test waveform, a sinus test waveform was defined. The appropriate limit forces were set between L_1=0.0300 N – L_2=0.3500 N, in order to secure that the specimen will not be exposed to load conditions that exceed the desired force. After a successful tuning was performed two different dynamic waveforms were implemented. First, a force controlled triangle wave was implemented, with force range that corresponds to the physiological pressure range (F_{low}=0.050 N – F_{high}=0.180 N) for 10 working cycles and at a frequency of f=1 Hz. In the following, a sinus wave was implemented with the same characteristics of the triangle wave (**Figure 2.13**).

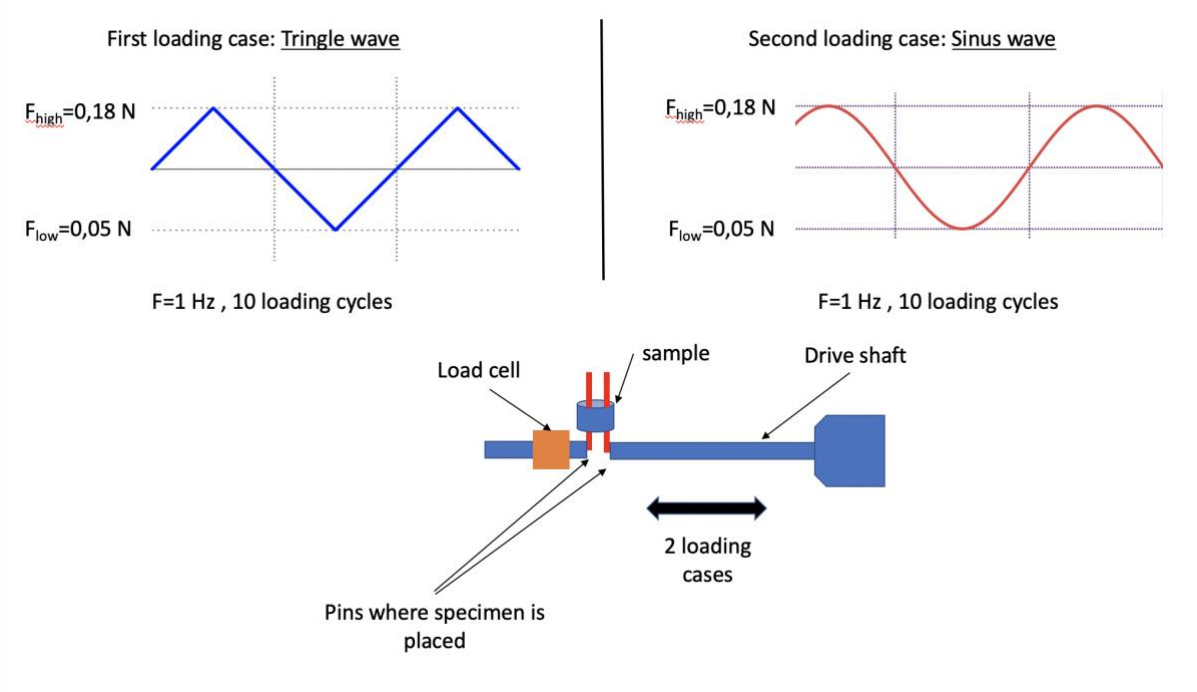

Figure 2.13: Characteristics of the two waves that were implemented for dynamic loading

For the DMA measurements, the data acquisition channels chosen were the displacement for the displacement channel, load for the load and the hold channel, since the goal were force controlled experiments. As sweep variable the frequency was chosen, with logarithmic increase from 1 Hz till 100 Hz with 5 points per decade. As for the mean level and dynamic amplitude control the load selection was selected. The load conditions were the following, hold value= 0.050 N, mean level= 0.180 N, dynamic amplitude= 0.150 N and the mean level rate was set

at MLR=0.1 N/sec. A representative of the DMA application after setting the desired conditions can be seen in **Figure 2.14** and **Figure 2.15**.

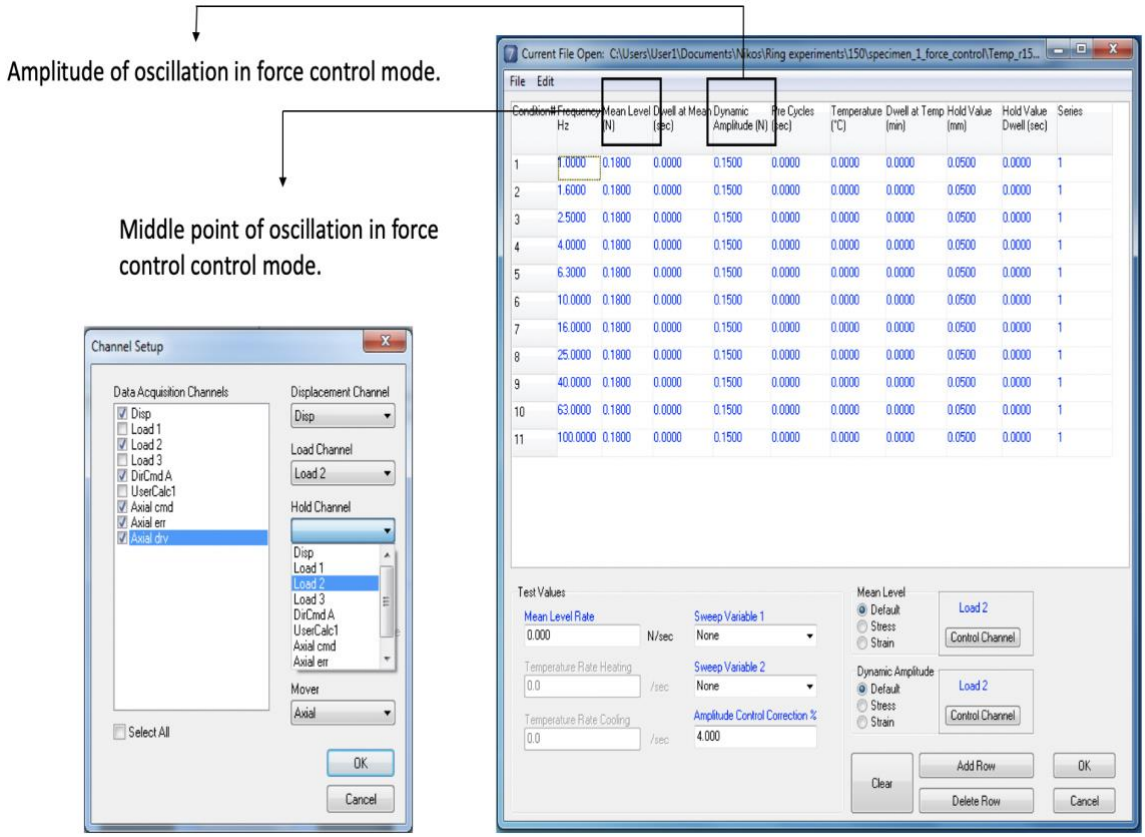

Figure 2.14: Typical windows of DMA application with desired constants for a logarithmic frequency sweep.

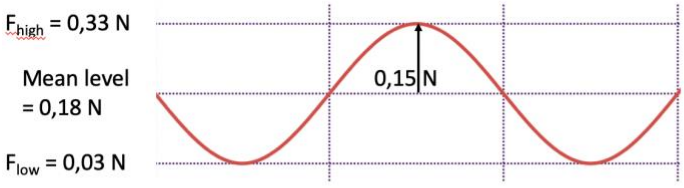

Dynamic Mechanical Analysis Measurement

Condition	Frequency (Hz)
1	1
2	1,6
3	2,5
4	4
5	6,3
6	10
7	16
8	25
9	40
10	63
11	100

Figure 2.15: Setting of the DMA measurements. Table with implemented frequencies and values set in WinTest®.

2.6.2 Strain calculation for cylindrical specimens

For the translation of the measured displacement of the mover to deformation of the specimen from the implemented force range, 2 different strain calculations were implemented as explained above.

1st Approach

The first approach for the evaluation of engineering strain was based on equation (2.6). The distance between the pins was translated into circumferential deformation of the specimen using Eqs. (2.7) - (2.9) [26]. The initial position of the pins was set 2 mm, after this the distance between the pins could be tracked in every position of the mover. In the position -4,60 mm of the mover the distance of the pins was 3 mm, which is equal to the theoretical inner diameter of the electrospun grafts. Based on this, the length of the inner circumference was calculated:

$$\varepsilon = \frac{\Delta L}{L_0} = \frac{C_m - C_0}{C_0} \quad (2.6)$$

$$C_{int} = \pi * \text{pin\_distance(3 mm)} \quad (2.7)$$

$$C_0 = \pi * \text{pin\_0\_distance(>3 mm)} \quad (2.8)$$

$$C_m = \pi * \text{pin\_m\_distance(> pin\_0\_distance)} \quad (2.9)$$

where, C_{int}: is the initial circumferencial length at position -4,60 mm, C_0: is the circumference at the starting position of the loading cycle, C_m: is the circumference at the maximum position of the loading cycle

The calculations of circumferential length were then used in equation 2.6 for the strain calculation.

2nd Approach

The second approach for the strain calculation was based on the same methodology with the first approach, but instead of using only the pin distance for the calculation of the circumference, the wall thickness (w.t) of the specimen is added. So, the equation 2.8 and 2.9 becomes:

$$C_0 = \pi * (\text{pin\_0\_distance} + \text{w.t}) \quad (2.10)$$

$$C_m = \pi * (\text{pin\_m\_distance} + \text{w.t}) \quad (2.11)$$

The new calculations of circumferential length were then used in equation 2.6 for the strain calculation.

Chapter 3

Results

In this section, the results obtained from the experiments mentioned in Chapter 2 are presented. The most important aspects for the evaluation of the implemented method for the structural characterization of electrospun vascular grafts is the reaction to the DMA experiments.

In all experiments, the handling of the electrospun grafts was critical. On the one hand, this is due to the extraction of the grafts from the metallic rods, on the other hand after the end of each DMA application the mover was returning on the initial position causing an overstretch of the specimens and as a result the destruction of the specimens. Nevertheless, a good amount of data has been achieved from the experiments that were performed and the analysis of these data produced results, that their significance is discussed in Chapter 4.

3.1 Open angle experiments

The measured open angles for the electrospun grafts with different wall thickness is shown in **Figure 3.1**. The mean and standard deviation of the opening angles were calculated for the specimens tested from each wall thickness. For the specimens with wall thickness 150μm, 200μm and 300μm the mean open angle was ~4.60º, ~1.78º and 9.55º respectively and the standard deviation was ~5.06º, ~1,90º, and ~4,04º.

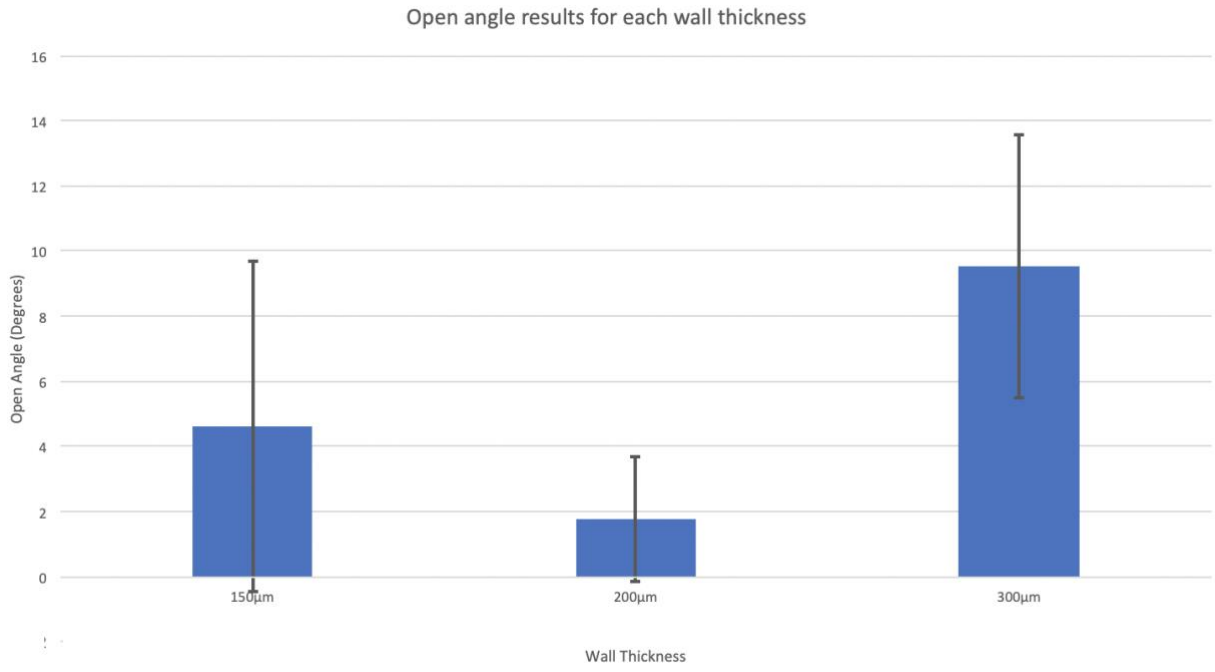

Figure 3.1: Measured opening angles of the grafts with different wall thickness. The three blue bars represent mean values. The black lines show the standard deviation.

The circumferential stretch ratios from the zero-stress to the no-load condition calculated on the specimens with three different wall thickness based on length measurements of the inner and outer wall are listed in **Table 3.1**.

Table 3.1: Calculated circumferential stretch ratios based on measured lengths of zero-stress and no-load states.

Wall Thickness	States	Length		Circumferential stretch ratios (λ_θ)	
		$(L^{i\theta})$ **Inner Wall (mm)**	$(L^{o\theta})$ **Outer Wall (mm)**	**Inner Wall** $(\lambda^{i\theta}_{no\ load})$	**Outer Wall** $(\lambda^{o\theta}_{no\ load})$
150μm	**Zero stress** $(L_{0\ stress})$	**8.08**	**8.67**	**1.006**	**1.013**
	No Load $(L_{no\ load})$	**8.12**	**8.78**		
200μm	**Zero stress** $(L_{0\ stress})$	**8.03**	**8.95**	**1.002**	**1.009**
	No Load $(L_{no\ load})$	**8.04**	**9.03**		
300μm	**Zero stress** $(L_{0\ stress})$	**8.04**	**9.33**	**0.99**	**1.009**
	No Load $(L_{no\ load})$	**8.03**	**9.41**		

No-load state indicates 0mmHg blood pressure. The circumferential stretch ratios, calculated values refer to zero-stress length measurements as explained in chapter 2.4.

The distribution of the circumferential residual stretch ratio in the vessel wall at the no-load condition for each wall thickness is illustrated in **Figure 3.2**. These values are the mean values of circumferential stretch ratio as it was measured from 5 specimens for each wall thickness. It is seen that the residual stretch ratio is tensile both in the inner and the outer wall. Under the conventional assumption that plane sections remain plane in bending, the stretch ratio distribution in the vessel wall is a straight line. In Figure 3.2B, the mean stretch ratio for electrospun grafts with wall thickness 200μm, is positive. The corresponding mean stretch ratio in the electrospun grafts with wall thickness of 300μm is shown in Figure 3.2C. It is seen that the residual stretch ratio is compressive in the inner wall and tensile in the outer wall.

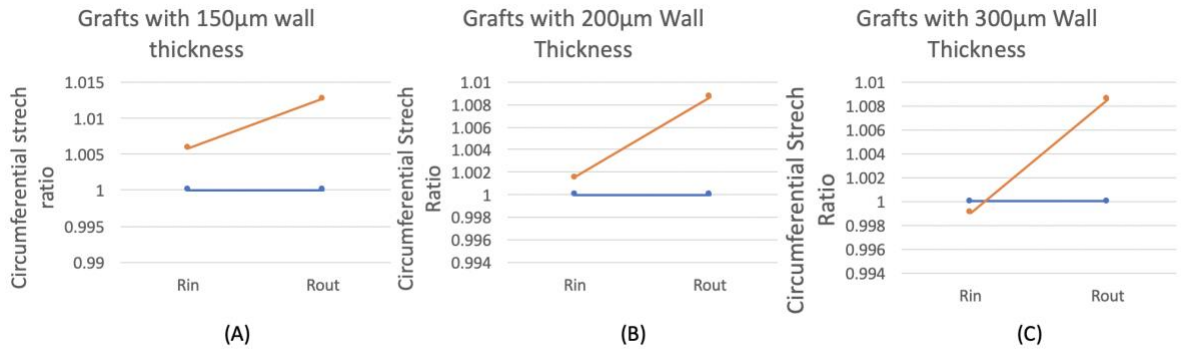

Figure 3.2: Circumferential stretch ratio distribution in the electrospun vessels whose dimensions are listed in Table 3.1. A: A mean measured residual stretch ratio for grafts with wall thickness of 150µm. Residual stretch can be read from linear scale shown on right. R_{in} and R_{out}, inner and outer radius of vessel wall, respectively. B: Mean circumferential stretch ratio at electrospun grafts with w.t of 200µm. C: corresponding stretch ratios of grafts with w.t of 300µm.

3.2 Deformation experiments

The effects of different wall thickness on the deformation of the ring-shaped grafts are shown in **Figure 3.3**. The blue line is for the ring with wall thickness of 150µm. The force starts rising after the ring has reached the stretched state, which is when the distance of the pins is 3,7 mm. To bring the ring in the stretched state it took a total displacement of 1,7 mm. For the same amount of displacement, the ring with wall thickness 200µm produced a force of $F_{stretched}$=0.05N. The ring with wall thickness of 300µm produced a force of $F_{stretched}$=0.24N, which already exceeds the physiological blood pressure range.

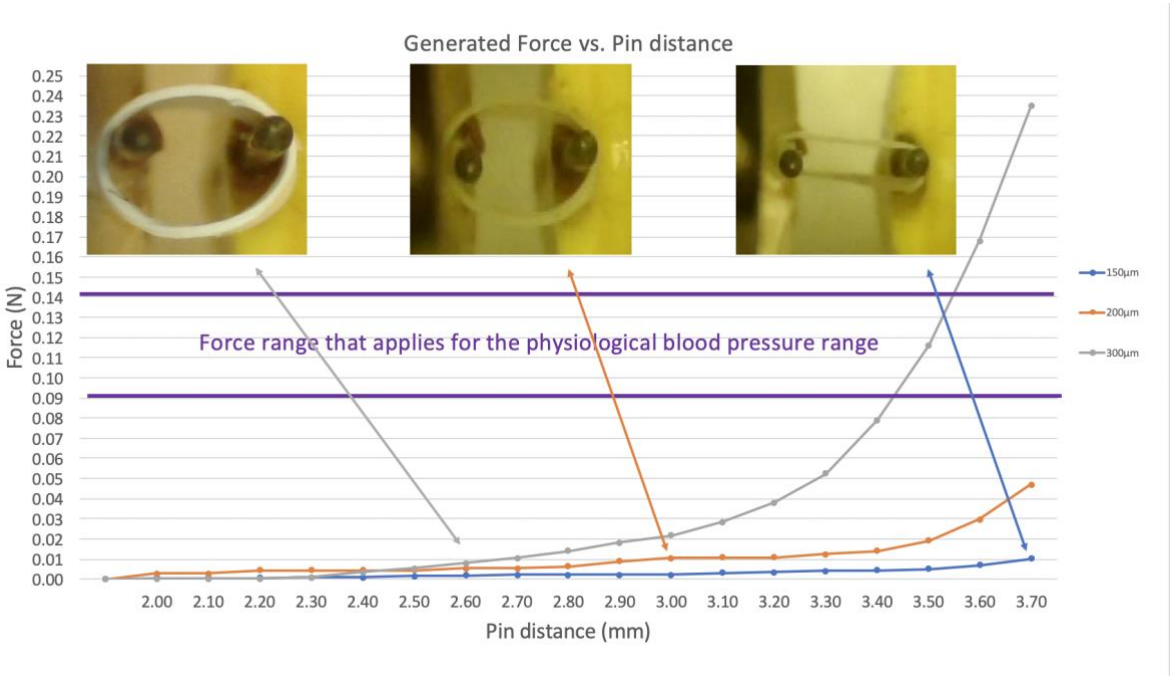

Figure 3.3: Generated force occurring from deforming three electrospun rings with different wall thickness. Blue line is for the ring with wall thickness of 150µm, the red for 200µm, and the green is for 300µm respectively. The violet lines depict the force range based on the physiological pressure range.

It can be seen that the three rings with different wall thickness produce a force greater than F_{min}=0,01 N at different points during the deformation process. For the ring with wall thickness of 300 μm this point is at the position -5,00 mm, where the pin distance is 2,6 mm which is less than the inner diameter of the grafts. For the ring with wall thickness of 200 μm F_{min} was reached at the position -4,60 mm, where the pin distance is 3 mm, equal to the inner diameter of the grafts. For the ring with wall thickness of 150μm F_{min} is reached at the position -3,90 mm, where the pin distance is equal to 3,7 mm.

3.3 Triangular loading & sinusoidal loading

The two loading cases, first the triangle wave and then the sinus wave, implemented at the beginning of the DMA workflow for preconditioning each specimen can be seen in **Figure 3.4**. These graphs contain results from only one specimen for each wall thickness and they are not average values for all the specimens tested. It can be seen, that although both waveforms were force controlled and implemented at the same force range (F_{low}=0.050 N – F_{high}=0.180 N), the result was different displacements at different positions through the working range. Furthermore, it can be seen that the unloading limit (lower limit) is decreasing in the graph of the triangle wave for each wall thickness.

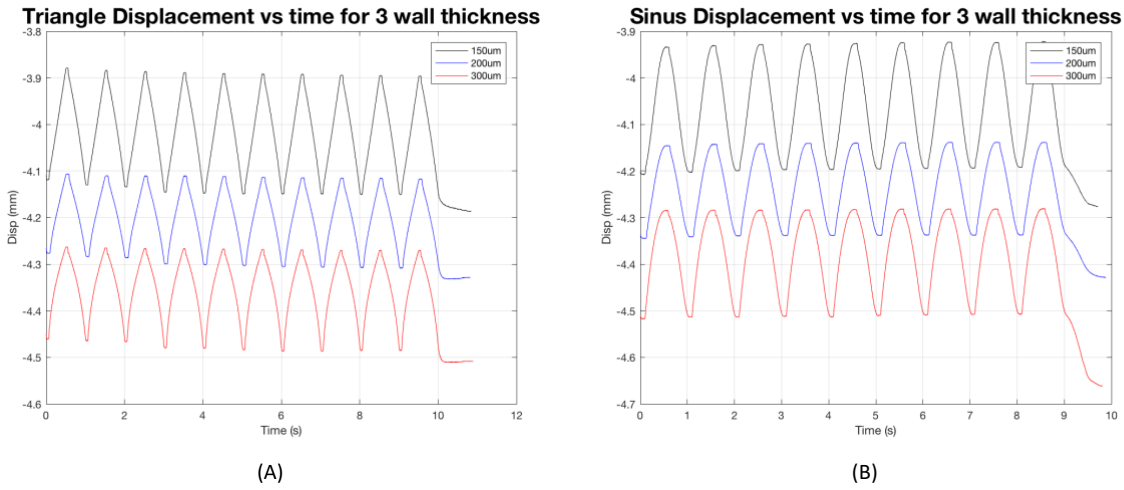

(A) (B)

Figure 3.4: The two waveforms, triangle (A) and sinus (B) versus Time, implemented for preconditioning of each specimen. Here can be seen the results only for a specimen of each wall thickness.

The Force-Displacement results from the two waveforms are presented in **Figure 3.5**. This graph is made from the data exported from the WinTest® software and displayed through Matlab. It can be seen that the implementation of the same force range at the electrospun grafts with different wall thickness produces displacement of the mover at different positions. The range of displacement is not identical for the triangular and sinusoidal waves. A further noticeable difference between the two implemented waveforms is the hysteresis loop that is produced from the cyclical loading of the specimen. In both graphs, the relationship between the load and displacement for the electrospun grafts with wall thickness of 300 & 200 μm is not linear. In contrast, the graph for the graft with 150 μm wall thickness seems to have a linear relation between the implemented force and generated displacement.

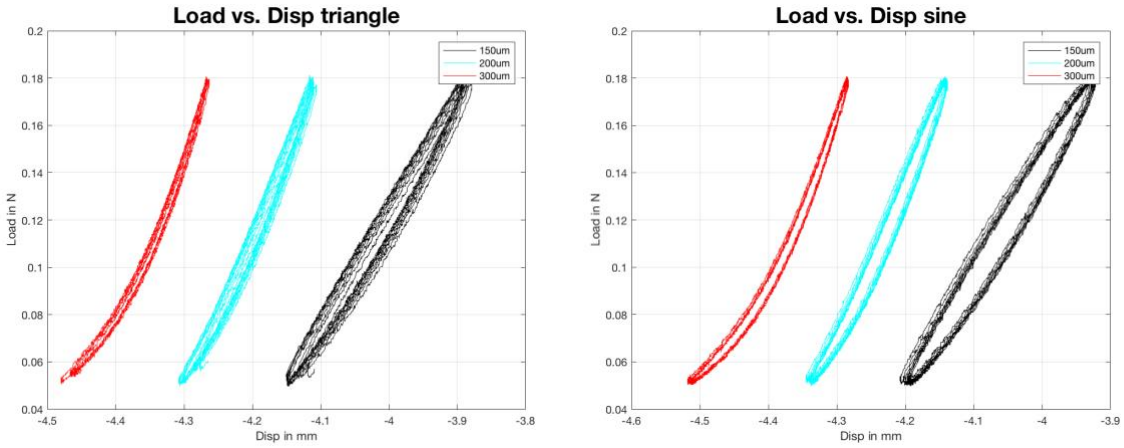

(A) (B)

Figure 3.5: The relationship between Load and Displacement for the electrospun grafts with different wall thickness for (A) the triangle wave and (B) the sinus wave.

In **Figure 3.6** are presented the stress-strain graphs, as they were calculated based on the first approach for strain calculation that is explained in the Materials & Methods section 2.6.2. More specifically, for the grafts with wall thickness 150 μm the produced stress was again 0.25 MPa in a corresponding strain of 10.5%. The maximum stress for the graft of wall thickness 200 and 300 μm was 0.15 MPa at 10% strain and 0.1 MPa at 8.8% strain respectively. Furthermore, the amplitude of strain corresponding to each stretched graph is decreasing with the wall thickness increasing. The values for the strain amplitudes resulted from the three methods are contained in **Table 3.2**.

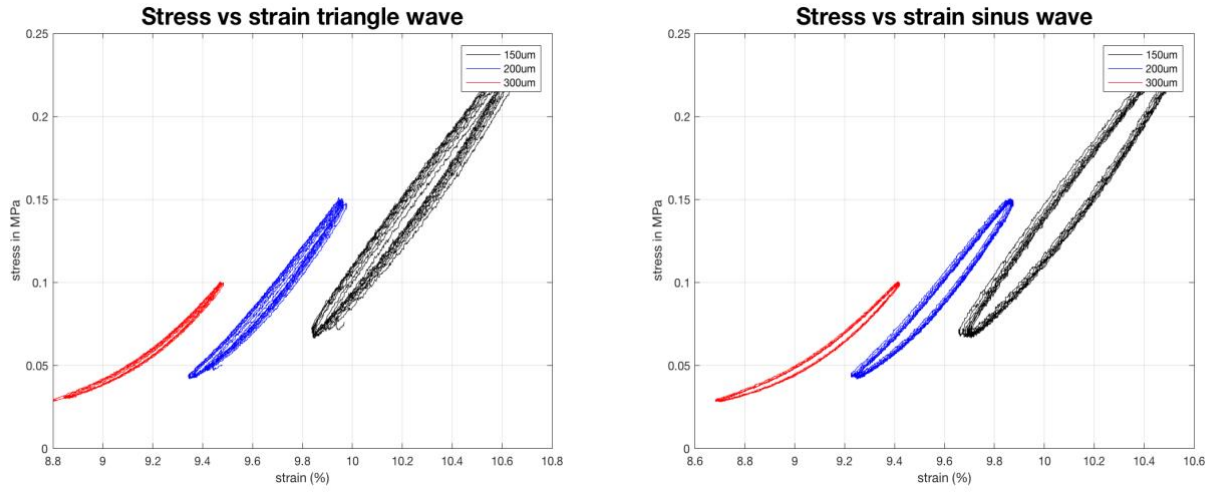

(A) (B)

Figure 3.6: The stress-strain curves for both waves implemented.

The results from the second calculation of strain, that include the wall thickness to the circumferential length calculation, are shown in **Figure 3.7**. In this case, the three graphs for specimens with different wall thickness line up. In contrast to **Figure 3.6**, the graphs are shifted in larger strains. Specifically, for the grafts with wall thickness 150 μm the maximum resulted stress is almost 0.25 MPa but with a corresponding strain of 11%, while with the second method

the same stress resulted at a strain of 10.5%. This implies a strain shift of 0.5% between the first and the second approach for strain calculation. This shift of strains increases for an increasing wall thickness of the graft being tested, for example the shift in strain of the grafts with wall thickness 200 and 300 μm is 0.6% and 0.9% respectively. The amplitude of the strains between the first and second approach of calculation is the same, as seen in **Table 3.2**.

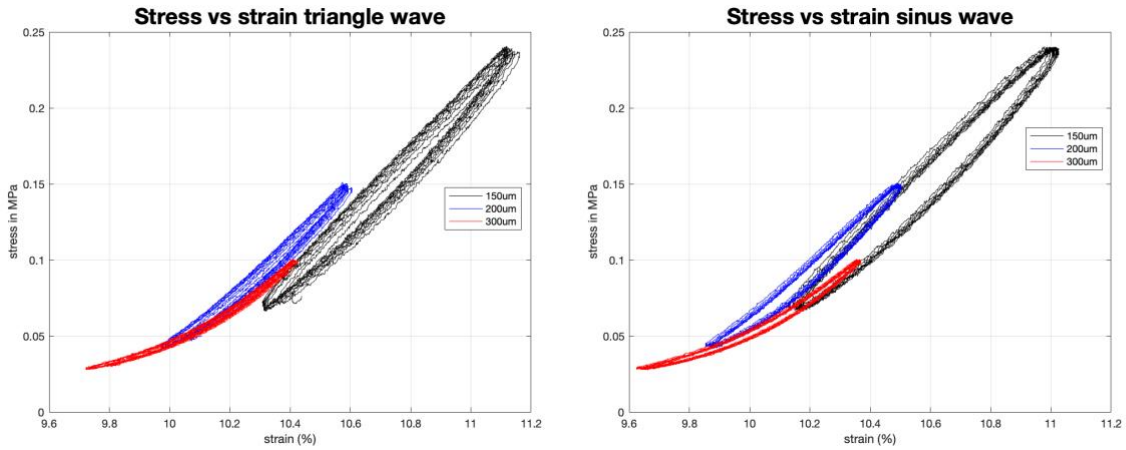

Figure 3.7: Stress-strain curves after concluding the wall thickness into the calculation of circumferential length.

Table 3.2: Strain amplitudes for each approach of strain calculation implemented.

	Strain calculation 1			**Strain calculation 2**		
	150 μm	**200 μm**	**300 μm**	**150 μm**	**200 μm**	**300 μm**
Strain Amplitude (%) **SINUS WAVE**	**0,85**	**0,61**	**0,71**	**0,85**	**0,60**	**0,70**
Strain Amplitude (%) **TRIANGLE WAVE**	**0,80**	**0,60**	**0,70**	**0,80**	**0,60**	**0,70**

The stress-strain curves in **Figure 3.7** were used to calculate the Elastic modulus at each loading cycle for both implemented waves, in order to compare the results between the dynamic loading at a single frequency and DMA with a frequency scan till 100 Hz. The resulted Elastic Modulus values from the dynamic loading waves implemented can be seen in **Figure 3.8**. The Elastic Modulus calculated from both waves are in close correlation. The Elastic Modulus values for the grafts with wall thickness of 150 and 200 μm were stable for the 8 loading cycles, in contrast for the graft with wall thickness 300 μm the Elastic modulus is not stable across the loading cycles implemented. The highest Elastic Modulus equals to 2.8 MPa and was observed for the grafts with wall thickness 150 μm. For the grafts with wall thickness 200 μm the calculated Elastic Modulus was 2.5 MPa.

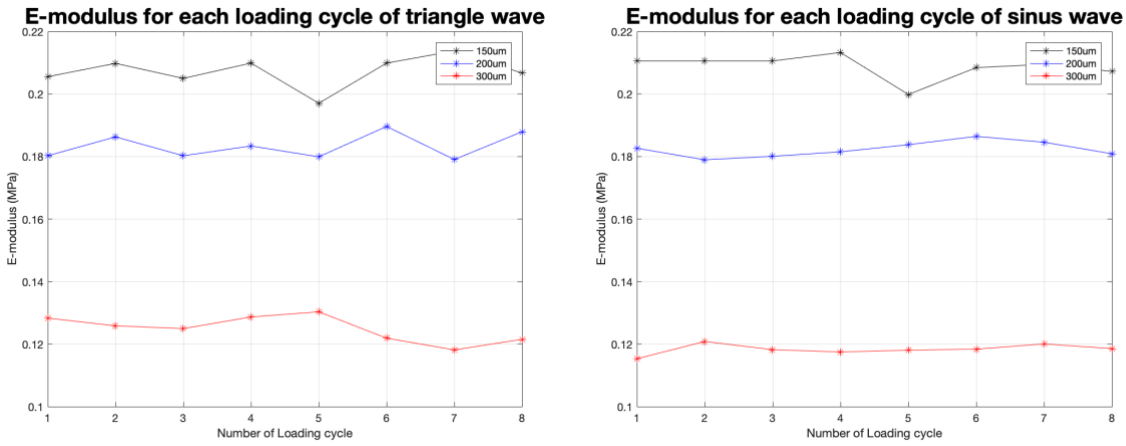

Figure 3.8: (A) Elastic Modulus from the implementation of triangle wave for 8 loading cycles in comparison to (B) Elastic Modulus calculated from sinus wave.

3.4 Results from DMA measurements

The application of a force controlled sinusoidal wave with logarithmically increasing frequency had different corresponding displacements for the grafts with different wall thickness, as it can be seen in **Figure 3.9**. The actual amplitude of force is between 0,10 N – 0,26 N instead of 0,03 N – 0,33 N, that was given as an input force range. Furthermore, it can be seen that the implementation of a force controlled wave resulted in displacements at different positions and with different displacement amplitudes.

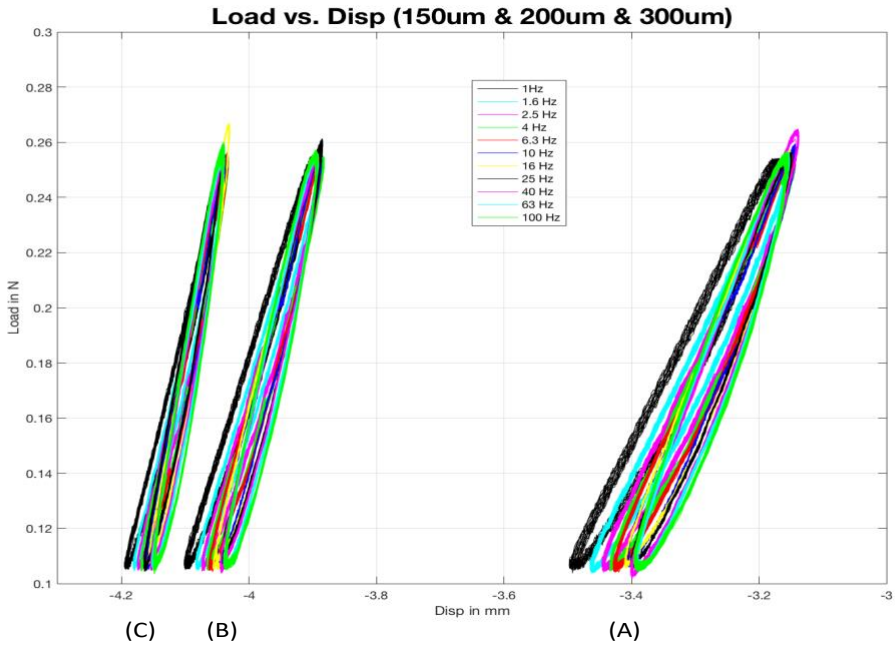

Figure 3.9: (A) The force-displacement graph for the grafts with 150 µm wall thickness. (B) & (C) are for the grafts with wall thickness of 200 µm & 300 µm respectively. Frequencies tested are shown with different colours.

The stress-strain graphs in **Figure 3.10** were calculated based on the force deformation curves in the figure above, and depending on the initial position of the mover when the loading cycle was beginning and on the amplitude of deformation. The same force range produced different stress values in the tested grafts. Specifically, for the grafts with wall thickness of 150 μm the maximum stress reached almost 0.35 MPa, while for the grafts with wall thickness 200μm and 300 μm the maximum stress reached was slightly above 0.2 MPa and above 0.15 MPa respectively. Moreover, while the max stress generated is stable over the frequency sweep the same it doesn't seem to apply for the generated strain. The increase of frequency in each step, increases the speed of mover, and the result is the stiffening of the grafts.

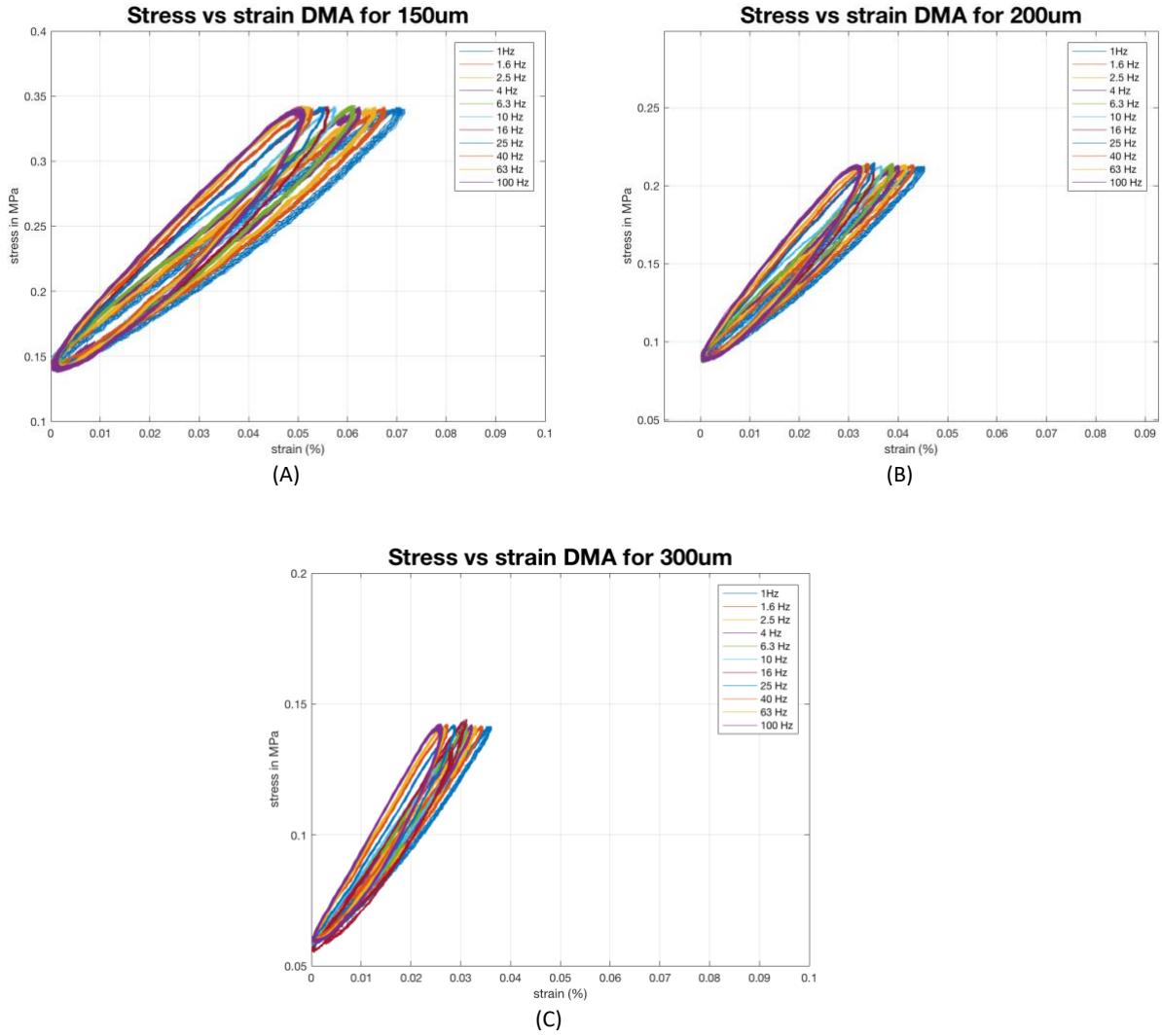

Figure 3.10: (A) Stress-strain relationship of grafts with wall thickness of 150μm for the frequency sweep. (B) & (C) the stress-strain for the grafts with wall thickness 200 μm and 300 μm.

As mentioned in the Introduction, the DMA measurements offer a variety of metrics for better understanding the structural properties of a specimen when it is subjected to a sinusoidal force wave with increasing frequency. Since in this case, the reference channel was force and the measured channel was displacement, the output was the dynamic stiffness together along with storage and loss stiffness. In **Figure 3.11** can be seen the results of the dynamic stiffness of the grafts across the frequency range tested. The graphs are separated depending on the wall thickness of the grafts. The graphs for 200 μm and 300 μm contain only four curves because 1 specimen from each wall thickness was destroyed due to failure of the DMA software. There is an increase of dynamic stiffness with increase of the frequency for all the specimens regardless the wall thickness. Moreover, there is an increase in the values of dynamic stiffness with increasing the wall thickness of the specimen tested, for the 150 μm samples the dynamic stiffness was from 0.5 – 0.8 N/mm, and for 200 and 300 μm samples was 0.8 – 1.2 N/mm and 0.9 – 1.4 N/mm respectively.

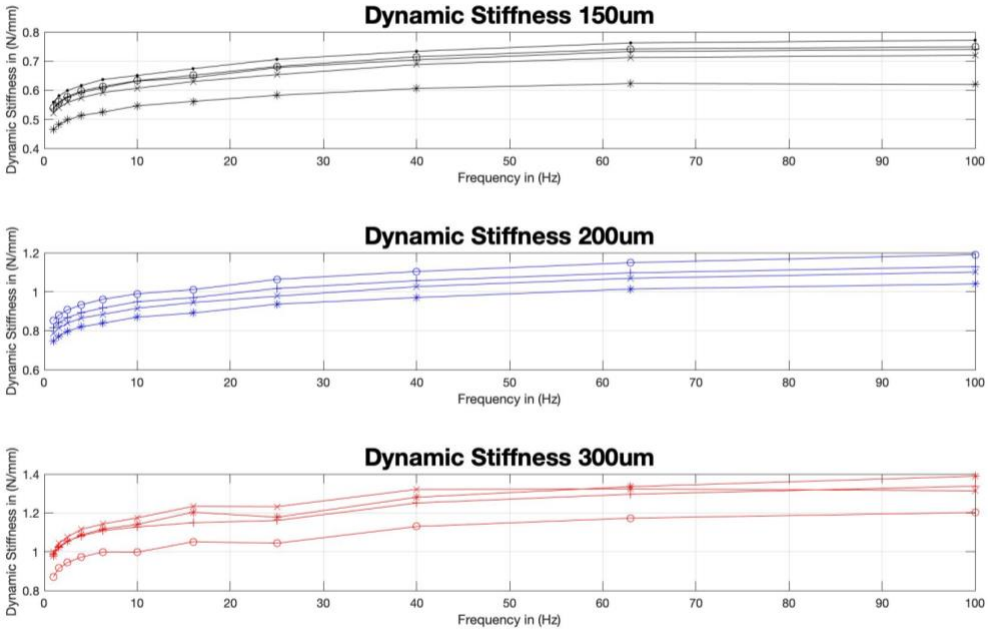

Figure 3.11: The Dynamic Stiffness of all the grafts tested.

In **Figure 3.12** the results for the storage stiffness of the specimens are very close to the values of the dynamic stiffness. Since the values of storage stiffness E' are very close to the dynamic stiffness E*, this is an indication that the specimens show more elastic behavior than viscous. The storage stiffness graphs show the same trends with the graphs of dynamic stiffness with increasing the storage stiffness while the frequency and the wall thickness increases. Together with the dynamic and the storage stiffness, the loss stiffness of the specimens is calculated and presented in the **Figure 3.13**. The highest values of loss stiffness, 0.9 – 1.35 N/mm, are observed for the samples with the thickest wall thickness and is increasing as the frequency increases.

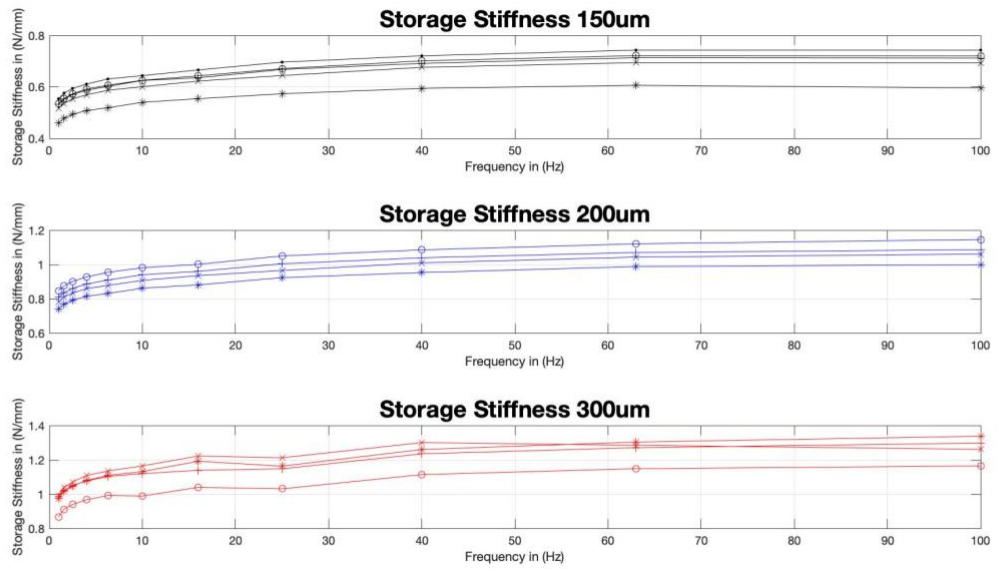

Figure 3.12: The storage Stiffness of all the grafts tested.

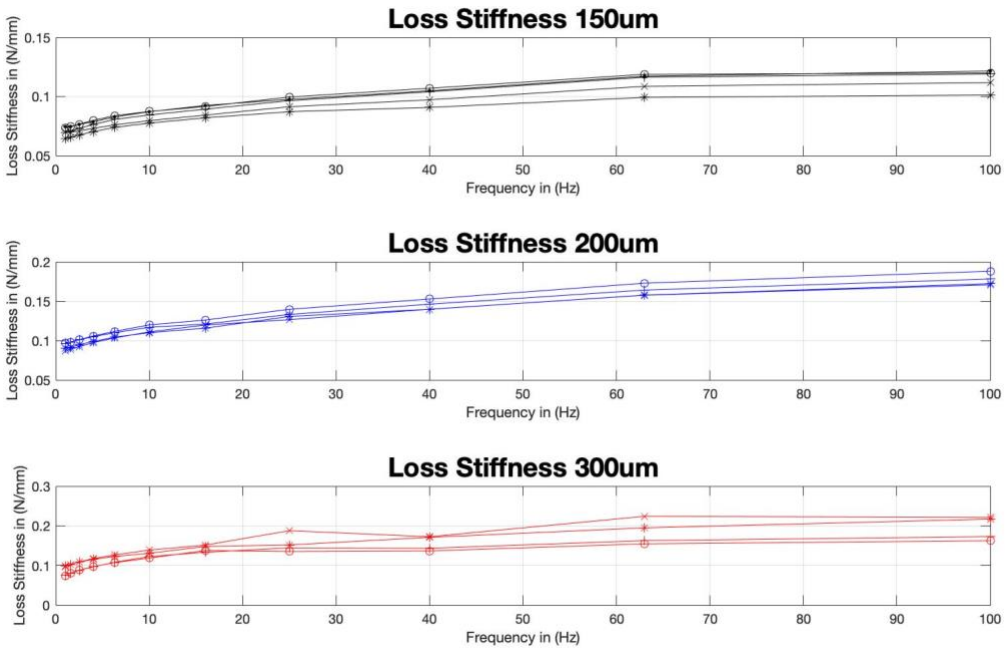

Figure 3.13: The Loss Stiffness of all the grafts tested.

The comparison between the stiffness metrics for the grafts with different wall thickness can be seen in **Figure 3.14**. These values represent mean values from all the grafts tested at each wall thickness. The increase of the wall thickness in the grafts results to an increase of the dynamic stiffness. The samples with 150 μm wall thickness had mean dynamic stiffness of 0,62 N/mm, while for 200 μm and 300 μm samples was 0,94 N/mm and 1,13 N/mm respectively.

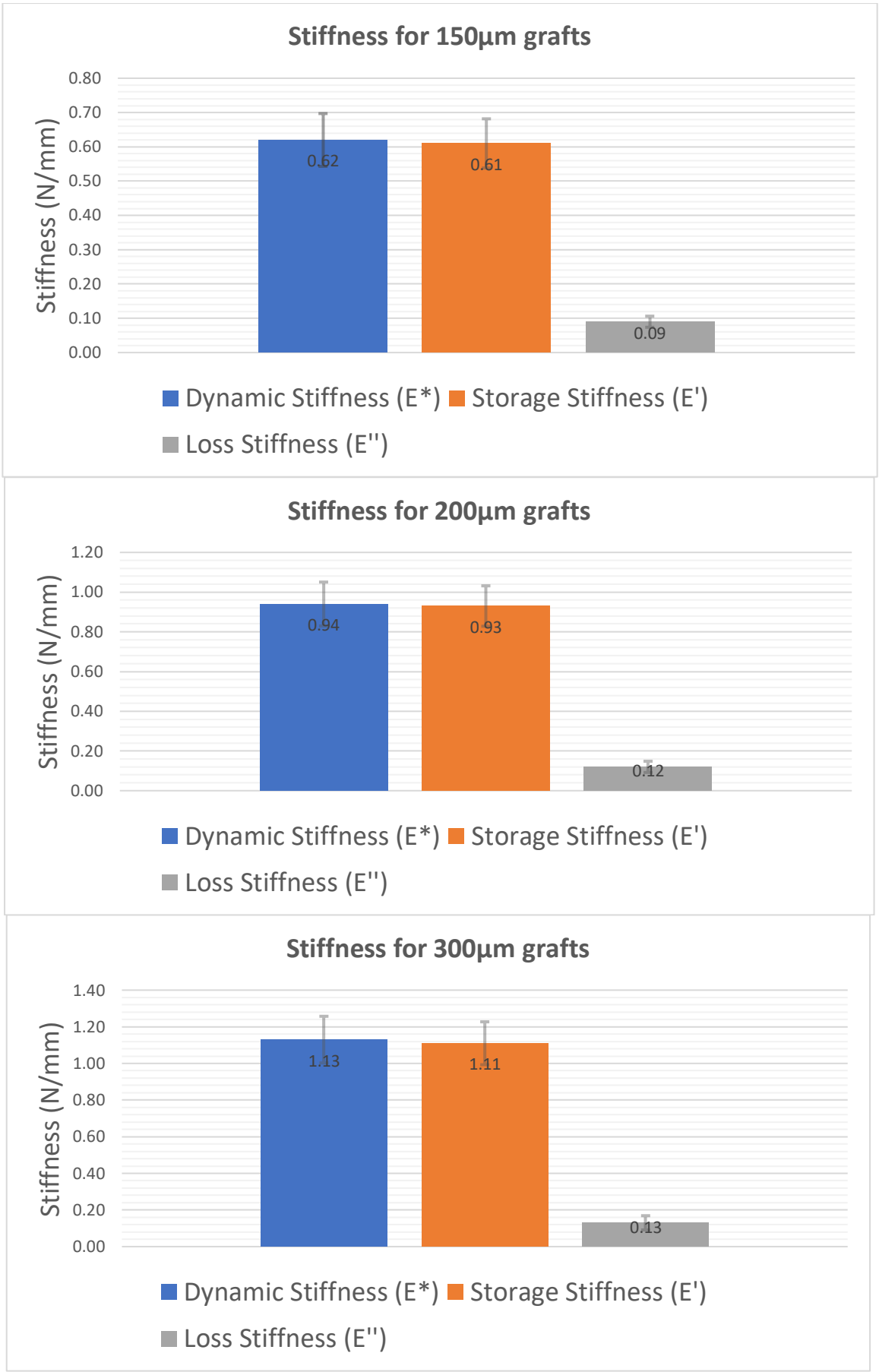

Figure 3.14: Comparison between stiffness for grafts with increasing wall thickness.

Another important measured value from the DMA software is the phase angle between the reference wave (force) applied, and the measured wave (displacement). The results can be seen in **Figure 3.15**. Three different graphs present the values of phase angle for the grafts with different wall thickness that were tested. At low frequencies, the thicker grafts present lower values of phase shift compared to the ones for the grafts with wall thickness of 150 μm, but at higher frequencies the phase shift values are comparable for all the grafts. The mean values of phase shift for the grafts can be compared in **Figure 3.16**. In contrast to the dynamic stiffness, the phase angle decreased as the wall thickness of the sample tested increased.

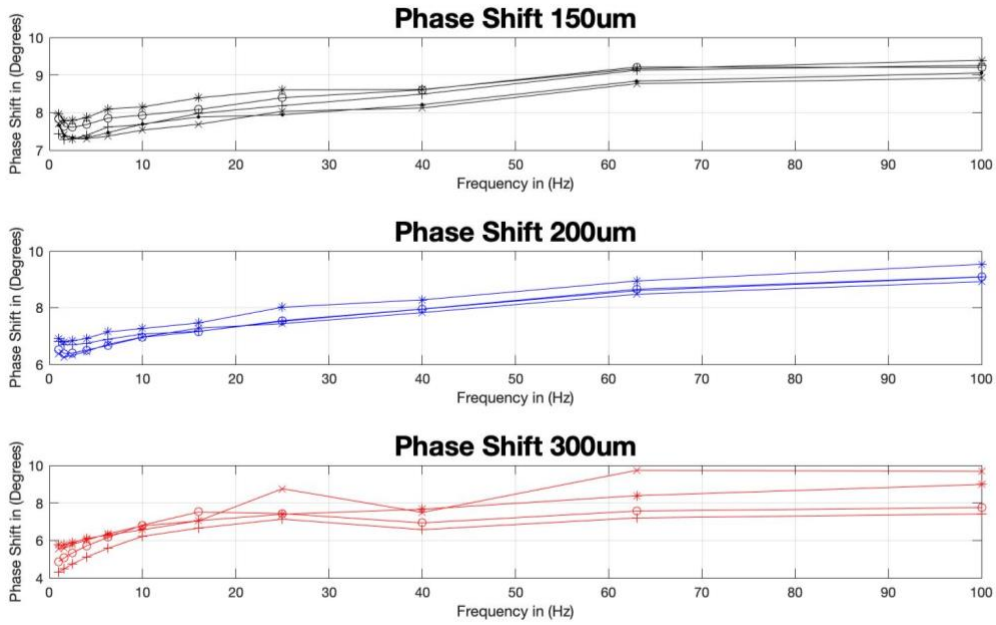

Figure 3.15: The Phase angle of all the grafts tested mechanically.

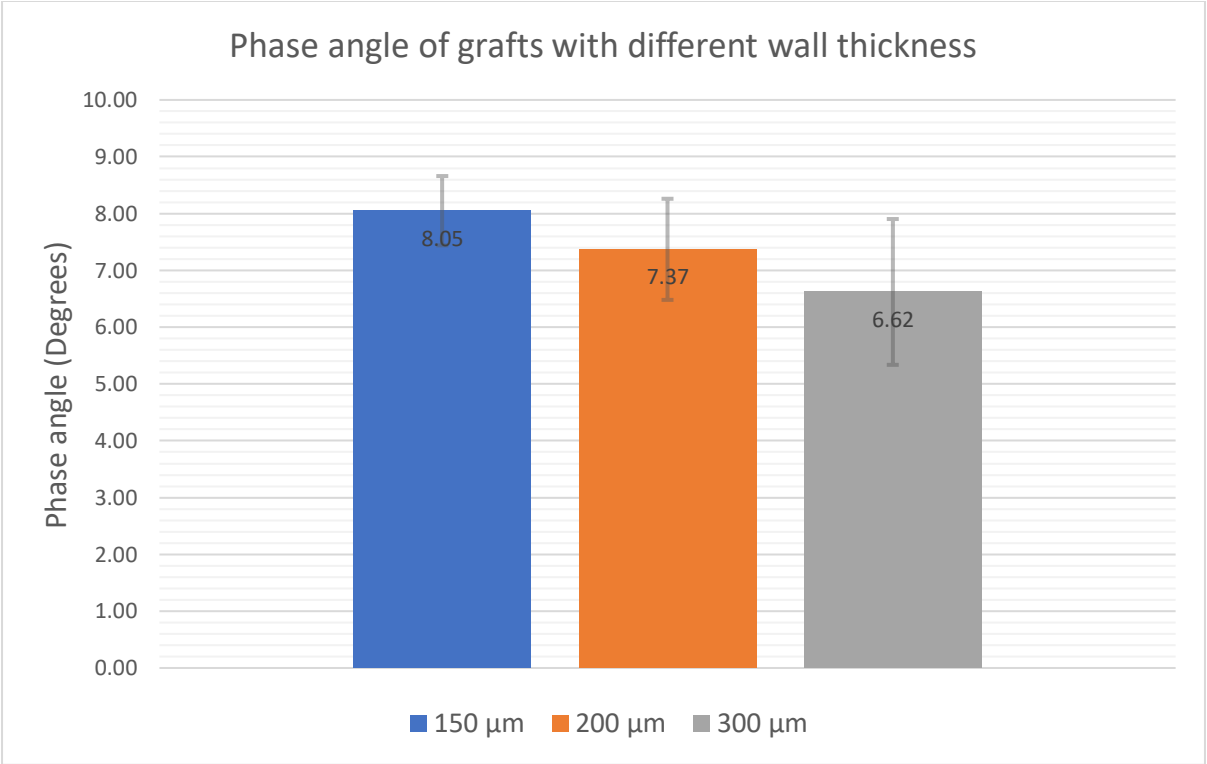

Figure 3.16: Comparison of mean phase angle for the grafts tested.

The impact of increasing frequency in the area of elastic hysteresis can be seen in **Figure 3.17**. The samples of wall thickness 150 µm and 200 µm showed a decrease in the area of the hysteresis loop at higher loading frequency. Also, the area of the hysteresis loop decreased at higher wall thickness (**Figure 3.18)**. Dissipated energy was 0.02 N*mm for samples of 150 µm, 0.01 N*mm for 200 µm and 0.008 N*mm for 300 µm.

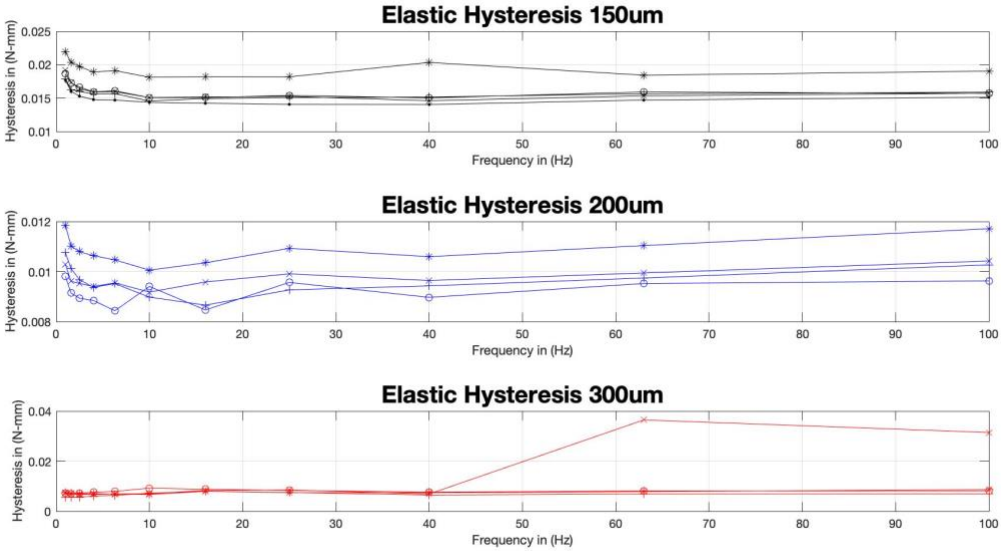

Figure 3.17: Elastic Hysteresis for the specimens with different wall thickness.

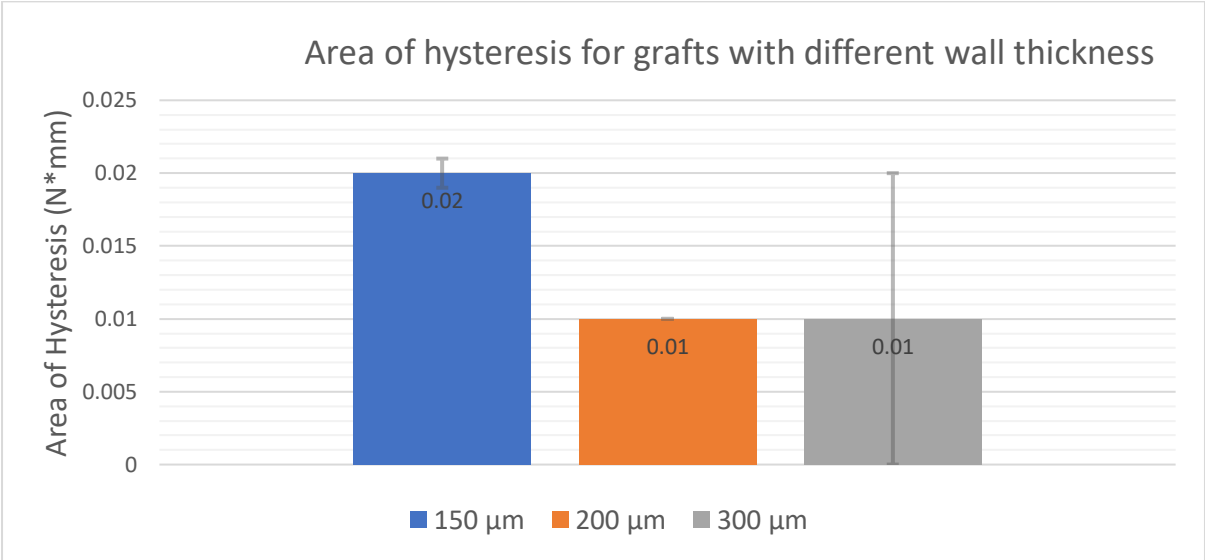

Figure 3.18: Comparison of mean values of area of Hysteresis loop for samples with different wall thickness.

At **Figure 3.19** is showed the measured tan delta for the samples with different wall thickness. Tan delta is the ratio of the loss modulus to the storage modulus and is a dimensionless value. In short, it is the ratio of viscous part to the elastic one in a polymer. The tan delta decreased at higher wall thickness (**Figure 3.20)**. DMA measurements showed that with increasing frequency, the tan delta increases also. For the 200 μm samples the values of tan delta were above 0.1 for lower frequencies and reached 0.15 for 100 Hz frequency.

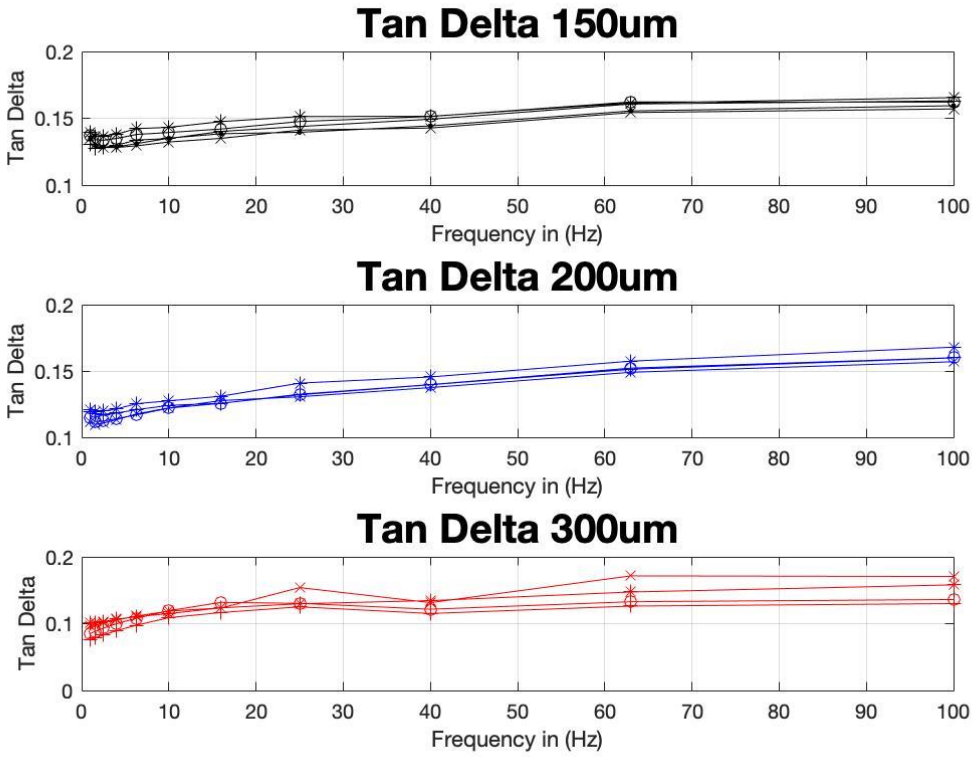

Figure 3.19: Tan Delta as it was measured from DMA measurements. It resembles the ratio between viscous and elastic part in the structure that was measured.

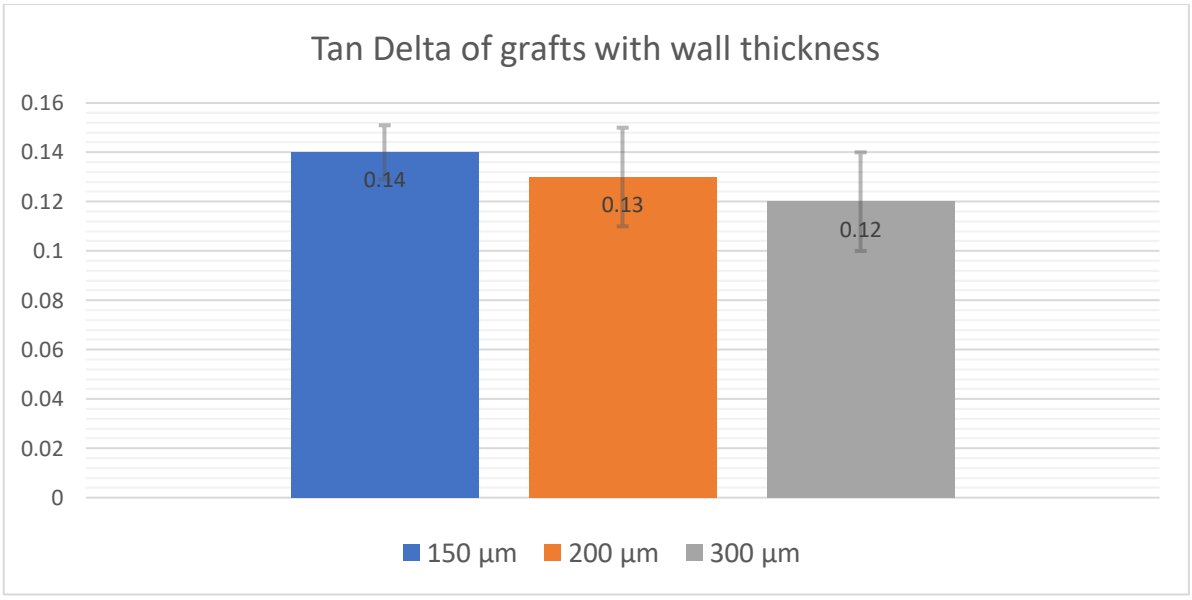

Figure 3.20: Mean values of Tan Delta for all the samples tested from each wall thickness

Chapter 4

Discussion

The aim of this thesis was the dynamic characterization of small-diameter electrospun vascular grafts at physiological pressure changes, by the use of DMA measurements and common dynamic loading experiments. Also, the effect of wall thickness to the mechanical characterization of ring-shaped specimens in tensile tests was evaluated. As shown in the results section the implementation of force controlled DMA measurements was successful in combination with dynamic loading for preconditioning of the specimens. From the 15 samples prepared for mechanical tests, five for each wall thickness produced, only one specimen from each graft with wall thickness of 200 μm and 300 μm was destroyed due to an error in the software that didn't allow to proceed four experiments in a row.

The results from the residual strain analysis show that as the wall thickness of the grafts increases, the distribution of the circumferential stretch ratio changes. For both grafts with wall thickness 150μm and 200μm the strain is tensile in both the inner and the outer wall, but this is not the case with the grafts of 300μm, where the strain is compressive in the inner wall region and tensile in the outer wall region. Although simple, the results for residual deformations based on the open angle experiments, provide qualitative information of the two-dimensional residual deformation.

Since the geometry of the ring-shaped specimens was the same, except the wall thickness, the displacement needed from the linear motor in order to bring the specimens into fully stretched position was assumed to be the same. From the deformation experiment can be derived that the parameter that affects the stiffness of the specimens is the wall thickness. The bigger the wall thickness of the specimen the higher is the force that is being produced from the deformation and this is a result from the bending of the fibers across the samples wall. As a consequence, the thickest samples exceed the force equivalent to physiological pressure values before it was fully stretched.

The common dynamic loading experiments showed that the application of specific waveform affects the area of the hysteresis loop. The area of the graph from the measurements with the sinus wave, which corresponds to the dissipated energy, is bigger than the area from the cycling loading with the triangle wave. The effect of increasing the wall thickness also affects the area of the hysteresis. The stress strain curves that were calculated show a non-linear relationship for the 300 μm samples. A possible explanation is that due to the high wall thickness the displacement applied did not result in actual deformation, and the generated force was a result from the bending of samples wall.

The results in section 3.3.2 show that DMA measurements are applicable for small ring-shaped electrospun samples. The structural behaviour of small diameter ring-shaped specimens was measured together with their dependency on loading frequency. More detailed information was gained from the DMA measurements in comparison to common dynamic loading experiments regarding the structural behaviour of the samples under physiological conditions.

4.1 Limitations

The limitations of this work are linked to the limits of the capabilities of the experimental equipment. The BOSE® Electroforce bench was unable to perform DMA experiments in Force control mode with Dynamic Amplitude smaller or equal to 0.1 N. Moreover, the system showed a resonance frequency at 50 Hz, which did not allow a linear frequency sweep and that was the reason why the logarithmic sweep was chosen.

Regarding the stress-strain calculation, the actual deformation of the samples was not possible to be measured. The size of the specimens did not allow the use of strain gauge for accurate strain measurements. The displacement of the mover was translated to two different strains that vary an order of magnitude from each other. An accurate measurement of the inner diameter of samples, after the extraction from the spinning rods, would lead to a more accurate calculation of strain and as a consequence to a better structural characterization.

4.2 Future goals

Despite their minor shortcomings, DMA measurements are applicable for small ring-shaped electrospun samples. In the future, it will be possible to further improve the measurements with a more sensitive load cell. Due to incapability to measure accurately the strain in the samples, the calculation gives a variance of an order of a magnitude. To increase the accuracy of the method, it would be necessary to stain the specimens and measure the actual deformation with a video extensometer. Due to the simplicity of the aforementioned method, improvements should be done also to the ambient conditions under which the measurements were performed. In order to be able to predict the mechanical behavior as it would occur in vivo, not only the forces that correspond to physiological pressure are essential, but the temperature and wettability are of vital importance.

4.3 Conclusion

The structural behavior of small diameter ring-shaped specimens was measured by DMA and compared to common dynamic loading tests. The measurements show that DMA is applicable for small ring-shaped electrospun samples. The viscoelasticity at varying frequencies at physiological loading was obtained, which gives more detailed information about the frequency dependent dynamic behavior. This allows a better characterization of the basic structural behavior in comparison to common dynamic tests.

References

[1] M. Nichols, N. Townsend, P. Scarborough, and M. Rayner, *European cardiovascular disease statistics*. 2012.

[2] T. J. Sill and H. A. von Recum, "Electrospinning: applications in drug delivery and tissue engineering," *Biomaterials*, vol. 29, no. 13, pp. 1989–2006, May 2008.

[3] Q. P. Pham, U. Sharma, and A. G. Mikos, "Electrospinning of polymeric nanofibers for tissue engineering applications: a review," *Tissue Eng.*, vol. 12, no. 5, pp. 1197–1211, May 2006.

[4] J. Doshi and D. H. Reneker, "Electrospinning process and applications of electrospun fibers," *J. Electrost.*, vol. 35, no. 2, pp. 151–160, Aug. 1995.

[5] L. Xue and H. P. Greisler, "Biomaterials in the development and future of vascular grafts," *J. Vasc. Surg.*, vol. 37, no. 2, pp. 472–480, Feb. 2003.

[6] T. Courtney, M. S. Sacks, J. Stankus, J. Guan, and W. R. Wagner, "Design and analysis of tissue engineering scaffolds that mimic soft tissue mechanical anisotropy," *Biomaterials*, vol. 27, no. 19, pp. 3631–3638, Jul. 2006.

[7] A. Formhals, "Formhals A 1934 US Patent no. 1975504," 1975504, 1934.

[8] D. I. Braghirolli, D. Steffens, and P. Pranke, "Electrospinning for regenerative medicine: a review of the main topics," *Drug Discov. Today*, vol. 19, no. 6, pp. 743–753, Jun. 2014.

[9] N. Bhardwaj and S. C. Kundu, "Electrospinning: A fascinating fiber fabrication technique," *Biotechnol. Adv.*, vol. 28, no. 3, pp. 325–347, May 2010.

[10] N. Awad, H. Niu, U. Ali, Y. Morsi, and T. Lin, "Electrospun Fibrous Scaffolds for Small-Diameter Blood Vessels: A Review," *Membranes*, vol. 8, no. 1, p. 15, Mar. 2018.

[11] M. M. L. Arras, C. Grasl, H. Bergmeister, and H. Schima, "Electrospinning of aligned fibers with adjustable orientation using auxiliary electrodes," *Sci. Technol. Adv. Mater.*, vol. 13, no. 3, p. 035008, Jun. 2012.

[12] M. Mohammadian and A. K. Haghi, "Systematic parameter study for nano-fiber fabrication via electrospinning process," p. 11.

[13] H. Bergmeister *et al.*, "Biodegradable, thermoplastic polyurethane grafts for small diameter vascular replacements," *Acta Biomater.*, vol. 11, pp. 104–113, Jan. 2015.

[14] H. Bergmeister *et al.*, "Healing characteristics of electrospun polyurethane grafts with various porosities," *Acta Biomater.*, vol. 9, no. 4, pp. 6032–6040, Apr. 2013.

[15] A. Hasan *et al.*, "Electrospun scaffolds for tissue engineering of vascular grafts," *Acta Biomater.*, vol. 10, no. 1, pp. 11–25, Jan. 2014.

[16] S. Sarkar, T. Schmitz-Rixen, G. Hamilton, and A. M. Seifalian, "Achieving the ideal properties for vascular bypass grafts using a tissue engineered approach: a review," *Med. Biol. Eng. Comput.*, vol. 45, no. 4, pp. 327–336, Apr. 2007.

[17] C. Grasl, H. Bergmeister, M. Stoiber, H. Schima, and G. Weigel, "Electrospun polyurethane vascular grafts: *In vitro* mechanical behavior and endothelial adhesion molecule expression," *J. Biomed. Mater. Res. A*, vol. 9999A, p. NA-NA, 2009.

[18] A. J. Pattison, M. McGarry, J. B. Weaver, and K. D. Paulsen, "A Dynamic Mechanical Analysis Technique for Porous Media," *IEEE Trans. Biomed. Eng.*, vol. 62, no. 2, pp. 443–449, Feb. 2015.

[19] D. Jones, "Dynamic mechanical analysis of polymeric systems of pharmaceutical and biomedical significance," *Int. J. Pharm.*, vol. 179, no. 2, pp. 167–178, Mar. 1999.

[20] P. Béhin, G. Stoclet, N. D. Ruse, and M. Sadoun, "Dynamic mechanical analysis of high pressure polymerized urethane dimethacrylate," *Dent. Mater.*, vol. 30, no. 7, pp. 728–734, Jul. 2014.

[21] K. P. Menard, *Dynamic mechanical analysis: a practical introduction*. Boca Raton, FL: CRC Press, 2008.
[22] "BOSE ElectroForce TestBench LM1." .
[23] "Instruction Manual optoCONTROL 2600.pdf." MICRO-EPSILON Eltrotec GmbH.
[24] C. J. Chuong and Y. C. Fung, "On Residual Stresses in Arteries," *J. Biomech. Eng.*, vol. 108, no. 2, p. 189, 1986.
[25] Y. C. Fung and S. Q. Liu, "Strain distribution in small blood vessels with zero-stress state taken into consideration," *Am. J. Physiol.-Heart Circ. Physiol.*, vol. 262, no. 2, pp. H544–H552, Feb. 1992.
[26] V. Laterreur *et al.*, "Comparison of the direct burst pressure and the ring tensile test methods for mechanical characterization of tissue-engineered vascular substitutes," *J. Mech. Behav. Biomed. Mater.*, vol. 34, pp. 253–263, Jun. 2014.

Appendix A

Matlab script for the stress-strain calculation of sinus and triangular waveforms

```
clc;

startingpoint= 4.600;
Lo= 7.48; %initial length of each specimen in mm
wt= [ 0.15; 0.200; 0.300]; %wall thicknesses in mm
r=0.3; %radius of pin
cycleVector=[ 1, 2, 3, 4, 5, 6, 7, 8];

% calculation of stress
for i=1:9001
    stress1(i)=load_sin_150(i)/0.75;
    stress2(i)=load_sin_200(i)/1.2;
    stress3(i)=load_sin_300(i)/1.8;
    stress1tri(i)=load_tri_150(i)/0.75;
    stress2tri(i)=load_tri_200(i)/1.2;
    stress3tri(i)=load_tri_300(i)/1.8;
end

% calculation of strain
for i=1:9001
    strain1(i)=abs(disp_sin_150(i)+abs(min(disp_sin_150)))/abs(min(disp_sin
_150));
    strain2(i)=abs(disp_sin_200(i)+abs(min(disp_sin_200)))/abs(min(disp_sin
_200));
    strain3(i)=abs(disp_sin_300(i)+abs(min(disp_sin_300)))/abs(min(disp_sin
_300));
    strain1tri(i)=abs(disp_tri_150(i)+abs(min(disp_tri_150)))/abs(min(disp_
tri_150));
    strain2tri(i)=abs(disp_tri_200(i)+abs(min(disp_tri_200)))/abs(min(disp_
tri_200));
    strain3tri(i)=abs(disp_tri_300(i)+abs(min(disp_tri_300)))/abs(min(disp_
tri_300));
end

%figure stress-strain sine wave
figure('Name','Stress vs Strain for 3 wall thickness')
plot(strain1,stress1,'k',strain2,stress2,'b',strain3,stress3,'r');
title('Stress vs strain sinus wave','FontSize',20);
xlabel('strain (%)');
ylabel('stress in MPa');
legend('150um','200um','300um');
axis([0 0.12 0 0.25]);
grid on;

%figure stress-strain triangle
figure('Name','Stress vs Strain for 3 wall thickness')
plot(strain1tri,stress1tri,'k',strain2tri,stress2tri,'b',strain3tri,stress3
tri,'r');
title('Stress vs strain triangle wave','FontSize',20);
xlabel('strain (%)');
ylabel('stress in MPa');
legend('150um','200um','300um');
axis([0 0.14 0 0.25]);
grid on;
```

```
%figure disp-time for sine wave
figure('Name','Disp vs time for sine wave')
plot(time_sin_150,disp_sin_150,'k',time_sin_200,disp_sin_200,'b',time_sin_3
00,disp_sin_300,'r');
title('Sinus Displacement vs time for 3 wall thickness','FontSize',20);
xlabel('Time (s)');
ylabel('Disp (mm)');
legend('150um','200um','300um');
grid on;

%figure disp-time for triangle wave
figure('Name','Disp vs time for triangle wave')
plot(time_tri_150,disp_tri_150,'k',time_tri_200,disp_tri_200,'b',time_tri_3
00,disp_tri_300,'r');
title('Triangle Displacement vs time for 3 wall thickness','FontSize',20);
xlabel('Time (s)');
ylabel('Disp (mm)');
legend('150um','200um','300um');
grid on;

%Function for the calculation of E-modulus for sinus wave of 3 w.t
[r_150_sin_E_modulus,r_200_sin_E_modulus,r_300_sin_E_modulus]=Emodcalculsin
(stress1,strain1,stress2,strain2,stress3,strain3);

%Function for the calculation of E-modulus for triangle wave of 3 w.t
[r_150_tri_E_modulus,r_200_tri_E_modulus,r_300_tri_E_modulus]=Emodcalculsin
(stress1tri,strain1tri,stress2tri,strain2tri,stress3tri,strain3tri);

%Plot the E-modulus for sinus wave of 3 w.t for each cycle.
figure('Name','E-modulus for sinus wave of 3 w.t for each cycle')
plot(cycleVector,r_150_sin_E_modulus,'*-
k',cycleVector,r_200_sin_E_modulus,'*-
b',cycleVector,r_300_sin_E_modulus,'*-r');
title('E-modulus for each loading cycle','FontSize',20);
xlabel('Number of Loading cycle');
ylabel('E-modulus (MPa)');
legend('150um','200um','300um');
grid on;

%Plot the E-modulus for triangle wave of 3 w.t for each cycle.
figure('Name','E-modulus for triangle wave of 3 w.t for each cycle')
plot(cycleVector,r_150_tri_E_modulus,'*-
k',cycleVector,r_200_tri_E_modulus,'*-
b',cycleVector,r_300_tri_E_modulus,'*-r');
title('E-modulus for each loading cycle','FontSize',20);
xlabel('Number of Loading cycle');
ylabel('E-modulus (MPa)');
legend('150um','200um','300um');
grid on;
```

Matlab script for making a figure for every metric calculated from DMA measurements

```
clc;


%graph for phase shift for each wall thickness for 5 specimens
figure('Name','Phase shift values of 3 wall thicknesses for  5 specimens')
subplot(3,1,1)
```

```
plot(frequencyVector, Delta150_1,'*-k',frequencyVector, Delta150_2,'+-
k',frequencyVector, Delta150_3,'o-k',frequencyVector,Delta150_4,'.-
k',frequencyVector, Delta150_5,'x-k');
title('Phase Shift 150um','FontSize',20);
xlabel('Frequency in (Hz)');
ylabel('Phase Shift in (Degrees)');
grid on;
subplot(3,1,2)
plot(frequencyVector, Delta200_1,'*-b',frequencyVector, Delta200_2,'+-
b',frequencyVector, Delta200_3,'o-b',frequencyVector, Delta200_5,'x-b');
title('Phase Shift 200um','FontSize',20);
xlabel('Frequency in (Hz)');
ylabel('Phase Shift in (Degrees)');
grid on;
subplot(3,1,3)
plot(frequencyVector, Delta300_1,'*-r',frequencyVector, Delta300_2,'+-
r',frequencyVector, Delta300_3,'o-r',frequencyVector, Delta300_4,'x-r');
title('Phase Shift 300um','FontSize',20);
xlabel('Frequency in (Hz)');
ylabel('Phase Shift in (Degrees)');
grid on;


%graph for Dynamic Stiffness for each wall thickness for 5 specimens
figure('Name','Dynamic Stiffness values of 3 wall thicknesses for  5
specimens')
subplot(3,1,1)
plot(frequencyVector, dynstiff150_1,'*-k',frequencyVector,
dynstiff150_2,'+-k',frequencyVector,dynstiff150_3,'o-
k',frequencyVector,dynstiff150_4,'.-k',frequencyVector, dynstiff150_5,'x-
k');
title('Dynamic Stiffness 150um','FontSize',20);
xlabel('Frequency in (Hz)');
ylabel('Dynamic Stiffness in (N/mm)');
grid on;
subplot(3,1,2)
plot(frequencyVector, dynstiff200_1,'*-b',frequencyVector,
dynstiff200_2,'+-b',frequencyVector, dynstiff200_3,'o-b',frequencyVector,
dynstiff200_5,'x-b');
title('Dynamic Stiffness 200um','FontSize',20);
xlabel('Frequency in (Hz)');
ylabel('Dynamic Stiffness in (N/mm)');
grid on;
subplot(3,1,3)
plot(frequencyVector, dynstiff300_1,'*-r',frequencyVector,
dynstiff300_2,'+-r',frequencyVector, dynstiff300_3,'o-r',frequencyVector,
dynstiff300_4,'x-r');
title('Dynamic Stiffness 300um','FontSize',20);
xlabel('Frequency in (Hz)');
ylabel('Dynamic Stiffness in (N/mm)');
grid on;


%graph for Hysteresis Loop for each wall thickness for 5 specimens
figure('Name','Hysteresis Loop values of 3 wall thicknesses for  5
specimens')
subplot(3,1,1)
plot(frequencyVector, Hysteresis150_1,'*-k',frequencyVector,
Hysteresis150_2,'+-k',frequencyVector,Hysteresis150_3,'o-
k',frequencyVector,Hysteresis150_4,'.-k',frequencyVector,
Hysteresis150_5,'x-k');
```

```
title('Elastic Hysteresis 150um','FontSize',20);
xlabel('Frequency in (Hz)');
ylabel('Hysteresis in (N-mm)');
grid on;
subplot(3,1,2)
plot(frequencyVector, Hysteresis200_1,'*-b',frequencyVector,
Hysteresis200_2,'+-b',frequencyVector, Hysteresis200_3,'o-
b',frequencyVector, Hysteresis200_5,'x-b');
title('Elastic Hysteresis 200um','FontSize',20);
xlabel('Frequency in (Hz)');
ylabel('Hysteresis in (N-mm)');
grid on;
subplot(3,1,3)
plot(frequencyVector, Hysteresis300_1,'*-r',frequencyVector,
Hysteresis300_2,'+-r',frequencyVector, Hysteresis300_3,'o-
r',frequencyVector, Hysteresis300_4,'x-r');
title('Elastic Hysteresis 300um','FontSize',20);
xlabel('Frequency in (Hz)');
ylabel('Hysteresis in (N-mm)');
grid on;


%graph for Loss Stiffness for each wall thickness for 5 specimens
figure('Name','Loss Stiffness values of 3 wall thicknesses for  5
specimens')
subplot(3,1,1)
plot(frequencyVector, lossstiff150_1,'*-k',frequencyVector,
lossstiff150_2,'+-k',frequencyVector,lossstiff150_3,'o-
k',frequencyVector,lossstiff150_4,'.-k',frequencyVector, lossstiff150_5,'x-
k');
title('Loss Stiffness 150um','FontSize',20);
xlabel('Frequency in (Hz)');
ylabel('Loss Stiffness in (N/mm)');
grid on;
subplot(3,1,2)
plot(frequencyVector, lossstiff200_1,'*-b',frequencyVector,
lossstiff200_2,'+-b',frequencyVector, lossstiff200_3,'o-b',frequencyVector,
lossstiff200_5,'x-b');
title('Loss Stiffness 200um','FontSize',20);
xlabel('Frequency in (Hz)');
ylabel('Loss Stiffness in (N/mm)');
grid on;
subplot(3,1,3)
plot(frequencyVector, lossstiff300_1,'*-r',frequencyVector,
lossstiff300_2,'+-r',frequencyVector, lossstiff300_3,'o-r',frequencyVector,
lossstiff300_4,'x-r');
title('Loss Stiffness 300um','FontSize',20);
xlabel('Frequency in (Hz)');
ylabel('Loss Stiffness in (N/mm)');
grid on;


%graph for Storage Stiffness for each wall thickness for 5 specimens
figure('Name','Storage Stiffness values of 3 wall thicknesses for  5
specimens')
subplot(3,1,1)
plot(frequencyVector, storstiff150_1,'*-k',frequencyVector,
storstiff150_2,'+-k',frequencyVector,storstiff150_3,'o-
k',frequencyVector,storstiff150_4,'.-k',frequencyVector, storstiff150_5,'x-
k');
title('Storage Stiffness 150um','FontSize',20);
```

```
xlabel('Frequency in (Hz)');
ylabel('Storage Stiffness in (N/mm)');
grid on;
subplot(3,1,2)
plot(frequencyVector, storstiff200_1,'*-b',frequencyVector,
storstiff200_2,'+-b',frequencyVector, storstiff200_3,'o-b',frequencyVector,
storstiff200_5,'x-b');
title('Storage Stiffness 200um','FontSize',20);
xlabel('Frequency in (Hz)');
ylabel('Storage Stiffness in (N/mm)');
grid on;
subplot(3,1,3)
plot(frequencyVector, storstiff300_1,'*-r',frequencyVector,
storstiff300_2,'+-r',frequencyVector, storstiff300_3,'o-r',frequencyVector,
storstiff300_4,'x-r');
title('Storage Stiffness 300um','FontSize',20);
xlabel('Frequency in (Hz)');
ylabel('Storage Stiffness in (N/mm)');
grid on;


%graph for Tan Delta for each wall thickness for 5 specimens
figure('Name','Tan Delta values of 3 wall thicknesses for  5 specimens')
subplot(3,1,1)
plot(frequencyVector, TanDelta150_1,'*-k',frequencyVector,
TanDelta150_2,'+-k',frequencyVector,TanDelta150_3,'o-
k',frequencyVector,TanDelta150_4,'.-k',frequencyVector, TanDelta150_5,'x-
k');
title('Tan Delta 150um','FontSize',20);
xlabel('Frequency in (Hz)');
ylabel('Tan Delta');
grid on;
subplot(3,1,2)
plot(frequencyVector, TanDelta200_1,'*-b',frequencyVector,
TanDelta200_2,'+-b',frequencyVector, TanDelta200_3,'o-b',frequencyVector,
TanDelta200_5,'x-b');
title('Tan Delta 200um','FontSize',20);
xlabel('Frequency in (Hz)');
ylabel('Tan Delta');
grid on;
subplot(3,1,3)
plot(frequencyVector, TanDelta300_1,'*-r',frequencyVector,
TanDelta300_2,'+-r',frequencyVector, TanDelta300_3,'o-r',frequencyVector,
TanDelta300_4,'x-r');
title('Tan Delta 300um','FontSize',20);
xlabel('Frequency in (Hz)');
ylabel('Tan Delta');
grid on;


%graph for Damping for each wall thickness for 5 specimens
figure('Name','Damping values of 3 wall thicknesses for  5 specimens')
subplot(3,1,1)
plot(frequencyVector, Damping150_1,'*-k',frequencyVector, Damping150_2,'+-
k',frequencyVector,Damping150_3,'o-k',frequencyVector,Damping150_4,'.-
k',frequencyVector, Damping150_5,'x-k');
title('Damping 150um','FontSize',20);
xlabel('Frequency in (Hz)');
ylabel('Damping');
grid on;
subplot(3,1,2)
```

```
plot(frequencyVector, Damping200_1,'*-b',frequencyVector, Damping200_2,'+-
b',frequencyVector, Damping200_3,'o-b',frequencyVector, Damping200_5,'x-
b');
title('Damping 200um','FontSize',20);
xlabel('Frequency in (Hz)');
ylabel('Damping');
grid on;
subplot(3,1,3)
plot(frequencyVector, Damping300_1,'*-r',frequencyVector, Damping300_2,'+-
r',frequencyVector, Damping300_3,'o-r',frequencyVector, Damping300_4,'x-
r');
title('Damping 300um','FontSize',20);
xlabel('Frequency in (Hz)');
ylabel('Damping');
grid on;
```

Matlab script for calculating the stress-strain curve from force-displacement for DMA measurements.

```
% This algorithm calculates the stress & strain for a DMA measurement and
% from the stress-strain graph calculate the Elastic Modulus.
clc;

for i=1:11
       if i==1
           for j=1:9001
               stress1(i,j)=load1_condition1(j)/0.75;
               strain1(i,j)=abs(disp1_condition1(j)+abs(min(disp1_condition
1)))/abs(min(disp1_condition1));
               stress2(i,j)=load2_condition1(j)/1.2;
               strain2(i,j)=abs(disp2_condition1(j)+abs(min(disp2_condition
1)))/abs(min(disp2_condition1));
               stress3(i,j)=load3_condition1(j)/1.8;
               strain3(i,j)=abs(disp3_condition1(j)+abs(min(disp3_condition
1)))/abs(min(disp3_condition1));
           end
       elseif i==2
           for j=1:9001
               stress1(i,j)=load1_condition2(j)/0.75;
               strain1(i,j)=abs(disp1_condition2(j)+abs(min(disp1_condition
2)))/abs(min(disp1_condition2));
               stress2(i,j)=load2_condition2(j)/1.2;
               strain2(i,j)=abs(disp2_condition2(j)+abs(min(disp2_condition
2)))/abs(min(disp2_condition2));
               stress3(i,j)=load3_condition2(j)/1.8;
               strain3(i,j)=abs(disp3_condition2(j)+abs(min(disp3_condition
2)))/abs(min(disp3_condition2));
           end
       elseif i==3
           for j=1:9001
               stress1(i,j)=load1_condition3(j)/0.75;
               strain1(i,j)=abs(disp1_condition3(j)+abs(min(disp1_condition
3)))/abs(min(disp1_condition3));
               stress2(i,j)=load2_condition3(j)/1.2;
               strain2(i,j)=abs(disp2_condition3(j)+abs(min(disp2_condition
3)))/abs(min(disp2_condition3));
               stress3(i,j)=load3_condition3(j)/1.8;
               strain3(i,j)=abs(disp3_condition3(j)+abs(min(disp3_condition
3)))/abs(min(disp3_condition3));
```

```
            end
        elseif i==4
            for j=1:9001
                stress1(i,j)=load1_condition4(j)/0.75;
                strain1(i,j)=abs(disp1_condition4(j)+abs(min(disp1_condition
4)))/abs(min(disp1_condition4));
                stress2(i,j)=load2_condition4(j)/1.2;
                strain2(i,j)=abs(disp2_condition4(j)+abs(min(disp2_condition
4)))/abs(min(disp2_condition4));
                stress3(i,j)=load3_condition4(j)/1.8;
                strain3(i,j)=abs(disp3_condition4(j)+abs(min(disp3_condition
4)))/abs(min(disp3_condition4));
            end
        elseif i==5
            for j=1:9001
                stress1(i,j)=load1_condition5(j)/0.75;
                strain1(i,j)=abs(disp1_condition5(j)+abs(min(disp1_condition
5)))/abs(min(disp1_condition5));
                stress2(i,j)=load2_condition5(j)/1.2;
                strain2(i,j)=abs(disp2_condition5(j)+abs(min(disp2_condition
5)))/abs(min(disp2_condition5));
                stress3(i,j)=load3_condition5(j)/1.8;
                strain3(i,j)=abs(disp3_condition5(j)+abs(min(disp3_condition
5)))/abs(min(disp3_condition5));
            end
        elseif i==6
            for j=1:9001
                stress1(i,j)=load1_condition6(j)/0.75;
                strain1(i,j)=abs(disp1_condition6(j)+abs(min(disp1_condition
6)))/abs(min(disp1_condition6));
                stress2(i,j)=load2_condition6(j)/1.2;
                strain2(i,j)=abs(disp2_condition6(j)+abs(min(disp2_condition
6)))/abs(min(disp2_condition6));
                stress3(i,j)=load3_condition6(j)/1.8;
                strain3(i,j)=abs(disp3_condition6(j)+abs(min(disp3_condition
6)))/abs(min(disp3_condition6));
            end
        elseif i==7
            for j=1:9001
                stress1(i,j)=load1_condition7(j)/0.75;
                strain1(i,j)=abs(disp1_condition7(j)+abs(min(disp1_condition
7)))/abs(min(disp1_condition7));
                stress2(i,j)=load2_condition7(j)/1.2;
                strain2(i,j)=abs(disp2_condition7(j)+abs(min(disp2_condition
7)))/abs(min(disp2_condition7));
                stress3(i,j)=load3_condition7(j)/1.8;
                strain3(i,j)=abs(disp3_condition7(j)+abs(min(disp3_condition
7)))/abs(min(disp3_condition7));
            end
        elseif i==8
            for j=1:9001
                stress1(i,j)=load1_condition8(j)/0.75;
                strain1(i,j)=abs(disp1_condition8(j)+abs(min(disp1_condition
8)))/abs(min(disp1_condition8));
                stress2(i,j)=load2_condition8(j)/1.2;
                strain2(i,j)=abs(disp2_condition8(j)+abs(min(disp2_condition
8)))/abs(min(disp2_condition8));
                stress3(i,j)=load3_condition8(j)/1.8;
                strain3(i,j)=abs(disp3_condition8(j)+abs(min(disp3_condition
8)))/abs(min(disp3_condition8));
            end
```

```
       elseif i==9
          for j=1:9001
               stress1(i,j)=load1_condition9(j)/0.75;
               strain1(i,j)=abs(disp1_condition9(j)+abs(min(disp1_condition
9)))/abs(min(disp1_condition9));
               stress2(i,j)=load2_condition9(j)/1.2;
               strain2(i,j)=abs(disp2_condition9(j)+abs(min(disp2_condition
9)))/abs(min(disp2_condition9));
               stress3(i,j)=load3_condition9(j)/1.8;
               strain3(i,j)=abs(disp3_condition9(j)+abs(min(disp3_condition
9)))/abs(min(disp3_condition9));
           end
       elseif i==10
           for j=1:9001
               stress1(i,j)=load1_condition10(j)/0.75;
               strain1(i,j)=abs(disp1_condition10(j)+abs(min(disp1_conditio
n10)))/abs(min(disp1_condition10));
               stress2(i,j)=load2_condition10(j)/1.2;
               strain2(i,j)=abs(disp2_condition10(j)+abs(min(disp2_conditio
n10)))/abs(min(disp2_condition10));
               stress3(i,j)=load3_condition10(j)/1.8;
               strain3(i,j)=abs(disp3_condition10(j)+abs(min(disp3_conditio
n10)))/abs(min(disp3_condition10));
           end
       else
          for j=1:9001
               stress1(i,j)=load1_condition11(j)/0.75;
               strain1(i,j)=abs(disp1_condition11(j)+abs(min(disp1_conditio
n11)))/abs(min(disp1_condition11));
               stress2(i,j)=load2_condition11(j)/1.2;
               strain2(i,j)=abs(disp2_condition11(j)+abs(min(disp2_conditio
n11)))/abs(min(disp2_condition11));
               stress3(i,j)=load3_condition11(j)/1.8;
               strain3(i,j)=abs(disp3_condition11(j)+abs(min(disp3_conditio
n11)))/abs(min(disp3_condition11));
           end
       end
end

   stress1=stress1';
   strain1=strain1';
   stress2=stress2';
   strain2=strain2';
   stress3=stress3';
   strain3=strain3';

%now i need to implement a function for the calculation of Emodulus in DMA.
%it will have as inputs the stress & strain matrixes and as an output the

%figure stress-strain for DMA measurement 150um
figure('Name','Stress vs Strain for 150um wall thickness for DMA
application')
plot(strain1,stress1);
title('Stress vs strain DMA for 150um','FontSize',20);
xlabel('strain (%)');
ylabel('stress in MPa');
legend('1Hz','1.6 Hz','2.5 Hz','4 Hz','6.3 Hz','10 Hz','16 Hz','25 Hz','40
Hz','63 Hz','100 Hz');
axis([0 0.10 0.10 0.40]);
hold on;
grid on;
```

```
%figure stress-strain for DMA measurement 200um
figure('Name','Stress vs Strain for 200um wall thickness for DMA
application')
plot(strain2,stress2);
title('Stress vs strain DMA for 200um','FontSize',20);
xlabel('strain (%)');
ylabel('stress in MPa');
legend('1Hz','1.6 Hz','2.5 Hz','4 Hz','6.3 Hz','10 Hz','16 Hz','25 Hz','40
Hz','63 Hz','100 Hz');
axis([0 0.10 0 0.25]);
hold on;
grid on;

%figure stress-strain for DMA measurement 300um
figure('Name','Stress vs Strain for 300um wall thickness for DMA
application')
plot(strain3,stress3);
title('Stress vs strain DMA for 300um','FontSize',20);
xlabel('strain (%)');
ylabel('stress in MPa');
legend('1Hz','1.6 Hz','2.5 Hz','4 Hz','6.3 Hz','10 Hz','16 Hz','25 Hz','40
Hz','63 Hz','100 Hz');
axis([0 0.10 0.05 0.20]);
hold on;
grid on;
```